AD-A110 873 MASSACHUSETTS INST OF TECH LEXINGTON LINCOLN LAB F/G 9/5
LARGE-SIGNAL CHARACTERIZATION, AMPLIFIER DESIGN, AND PERFORMANC--ETC(U)
DEC 81 C D BERGLUND F19628-80-C-0002
UNCLASSIFIED TR-586 ESD-TR-81-296 NL

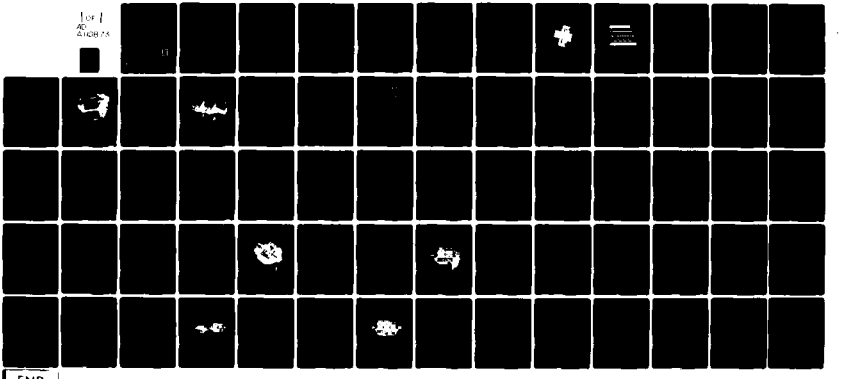

END
DATE FILMED
DTIC

ESD-TR-81-296

Technical Report	586
Large-Signal Characterization, Amplifier Design, and Performance of K-Band GaAs MESFETS	C.D. Berglund A 11 December 1981

Prepared for the Department of the Air Force
under Electronic Systems Division Contract F19628-80-C-0002 by

Lincoln Laboratory

MASSACHUSETTS INSTITUTE OF TECHNOLOGY

LEXINGTON, MASSACHUSETTS

The work reported in this document was performed at Lincoln Laboratory, a center for research operated by Massachusetts Institute of Technology, with the support of the Department of the Air Force under Contract F19628-90-C-0002.

This technical report has been reviewed and is approved for publication.

FOR THE COMMANDER

Raymond L. Loiselle

Raymond L. Loiselle, Lt.Col., USAF
Chief, ESD Lincoln Laboratory Project Office

MASSACHUSETTS INSTITUTE OF TECHNOLOGY
LINCOLN LABORATORY

LARGE-SIGNAL CHARACTERIZATION, AMPLIFIER DESIGN, AND PERFORMANCE OF K-BAND GaAs MESFETS

C.D. BERGLUND
Group 63

TECHNICAL REPORT 586

11 DECEMBER 1981

LEXINGTON MASSACHUSETTS

ABSTRACT

Recent advances in Gallium Arsenide field-effect transistor technology have extended the power amplification capabilities of FETs to the K-Band frequency range. FETs with performance capability of 0.5 watt power output at 20 GHz have been developed. Large-signal S-parameter characterizations of these devices have been utilized in designing power amplifiers. Transistor performance capability is discussed together with the performance of experimental amplifier designs realized in a microstrip environment.

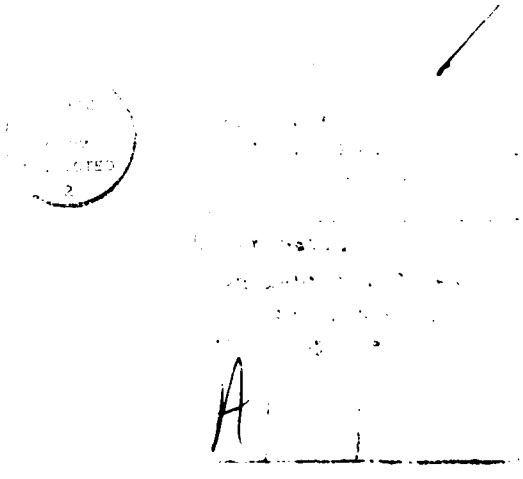

CONTENTS

I. INTRODUCTION

A program to develop K-Band field effect transistors for use in power amplifier stages of an EHF satellite downlink transmitter has produced FETs with 0.5 watt power output capability at 20 GHz. Successful utilization of these FETs in power amplifiers is greatly enhanced by large signal characterizations of the transistor. Consequently, techniques for characterizing K-Band FETs and designing amplifier circuits have been developed (in parallel with device development). This report describes a procedure for obtaining a large-signal S-parameter description of the transistor including "The Two Signal Method Of Measuring S-Parameters".[1] An appropriate error-correction model is implemented via computer-aided measurement and modeling to further improve the accuracy of these characterizations. Amplifier design procedure is discussed in conjunction with transistor characterizations for amplifiers realized in a microstrip environment. The performance of these FETs in the microstrip environment and in complete amplifier stages is reported.

II. TRANSISTOR DEVELOPMENT

A K-Band field-effect transistor development program was awarded to Microwave Semiconductor Corporation of Somerset, New Jersey in July 1979. The goals of this program were as listed below.

TABLE I

PERFORMANCE SPECIFICATIONS FOR K-BAND 0.5 W FET

Performance At 21 GHz	Goal	Minimum
Power Output	1.0 watt	0.5 watt
Power Added Efficiency	20%	15%
Gain	5.0 dB	4.0 dB
Junction Temperature Rise Corresponding To Above Performance		$\leq$ 100°C
Deliverables	50 Transistors	
Estimated Program Duration	9 Months	

MSC's approach to meeting these requirements consisted essentially of modifying an existing product, the MSC 88200 series Ku-Band transistor, to extend its frequency of operation to 21 GHz[2]. The Gallium Arsenide MESFET which resulted from this modification is shown in Fig. 1A and 1B. It employs a flip-chip configuration, self-aligned gates, and uses plated sources to make ground connections[3]. Sixteen gates with lengths of either 1.0 μm or 0.7 μm provide a total gate width of 1200 μm. The transistor chip is mounted on a metal base (chip-carrier) which includes alumina standoffs and leads to provide ease of installation in circuitry. These devices typically exhibit a pinchoff of $\approx$ 7 volts, saturation current of $\approx$ 350 mA, and very low thermal resistance ($\leq$ 15°C/W as measured by IR radiometric microscope) which makes them an excellent candidate for high-reliability applications.

MSC met requirements in contract deliverables with nominal FET performance in the vicinity of the specifications[4]. FET performance is discussed in

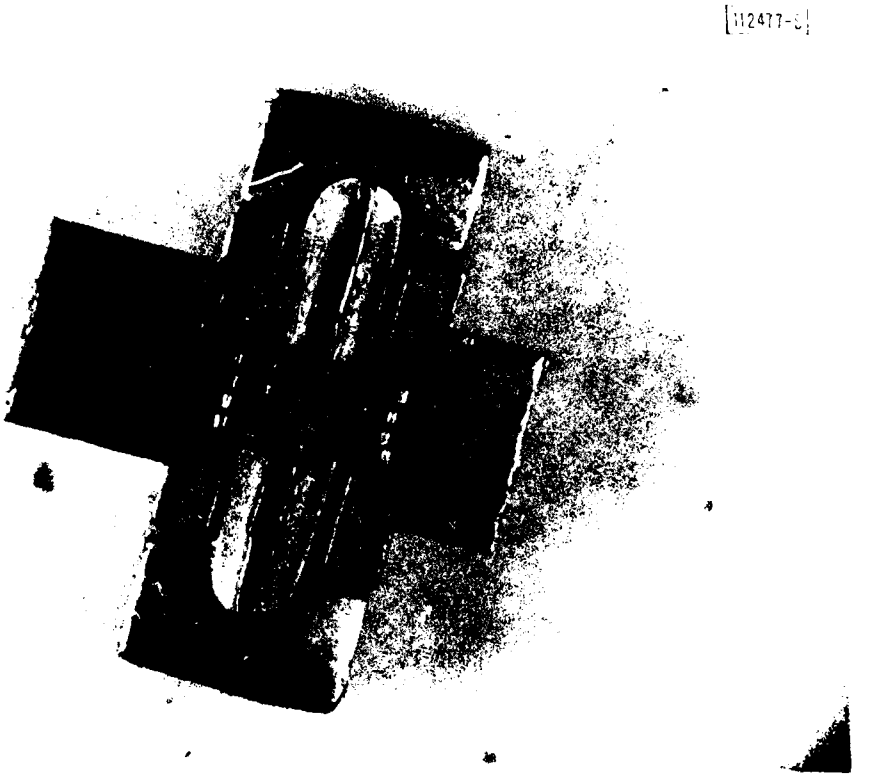

Fig. 1A. K-band 0.5 W GaAs MESFET package.

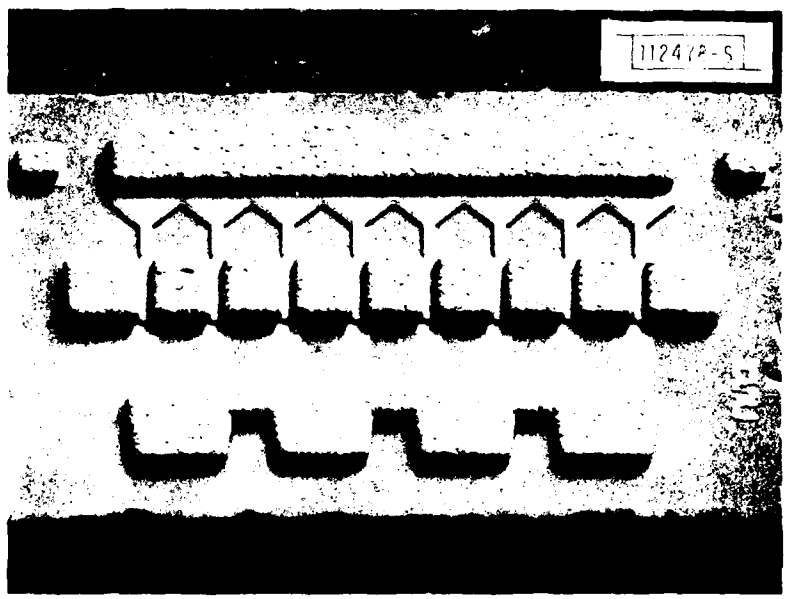

Fig. 1B. K-band 0.5 W GaAs MESFET chip.

more detail later in this report. In addition, MSC has provided additional K-Band FETs for purchase in a quantity similar to that of the contract requirements. In conjunction with FET development, techniques for characterizing transistors and designing amplifier circuitry have been developed at Lincoln Laboratory. The development effort employing microstrip circuitry is reported here; alternative techniques are reported elsewhere[5].

III. DEVICE CHARACTERIZATION AND CIRCUIT DESIGN PROCEDURE

S-parameter characterization of the field-effect transistors is accomplished with computer controlled network analyzer instrumentation. Complete two-port error-correction capability of measured data is provided by appropriate software and measurement standards. The twelve-element error model which is utilized is shown in Figs. 2A and B together with the appropriate defining equations. It is essentially that described by Staecker, modified here to include leakage terms, and is similar to that reported by Rehnmark[6]. Equations (1) through (16) relate error parameters to the complex wave variables and power-flow variables for the complete two-port error model. Error parameters E_{00}, E_{11}, and $E_{01}\,E_{10}$ (or E_{33}, E_{22}, and $E_{23}E_{32}$) are obtained from a minimum of three reflection measurements using a reference and offset shorts ($S_{21} = S_{12} = 0$). Transmission measurement with $S_{21} = S_{12} = 0$ yields parameters E_{30} and E_{03}; E_{44} and E_{32} (or E_{55} and E_{01}) are determined from measurement of a through connection ($S_{21} = S_{12} = 1$ and $S_{11} = S_{22} = 0$). The reflected and transmitted signals (X_{1R}, X_{1T}, X_{2R}, X_{2T}) for the device under test are then measured with respect to the reference signal, and equations (13) through (16) are solved to obtain the scattering parameters of the device under test.

Microstrip measurement standards and test-holders were designed to permit calibration of the measurement system at the transistor terminals. The microstrip transmission medium was selected for use because of its physical compatibility with the FET "package". The microstrip environment is well-suited for amplifier applications with its inherent small size, light weight, and ease of production. Transistor characterizations in the microstrip holder provide criteria for microstrip-amplifier design which avoid parasitics at the circuit-transistor interface which may be introduced by test holders designed in other mediums. The test-holder provides a 50-ohm environment in which to measure the transistor S-parameters (Fig. 3). The FET is held in place by a mechanical fixture which provides the flexibility of easy FET removal for testing in other circuitry. The mechanical fixture (see Fig. 21) permits pressure to be applied by an adjustable screw to an insulating bushing which presses the FET leads

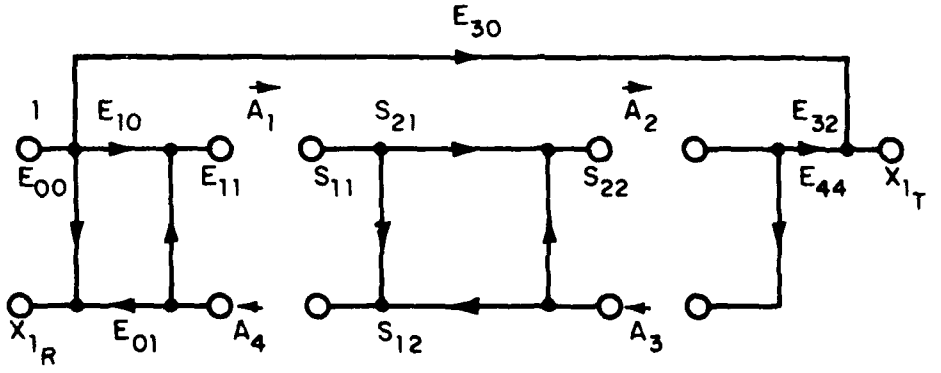

(1) $A_1 = E_{10} + E_{11}\ A_4$

(2) $A_3 = E_{44} A_2$

(3) $X_{1_R} = E_{00} + E_{01}\ A_4$

(4) $X_{1_T} = E_{32}\ A_2 + E_{30}$

(5) $A_4 = S_{11}\ A_1 + S_{12}\ A_3$

(6) $A_2 = S_{21}\ A_1 + S_{22}\ A_3$

112494-N

Fig. 2A. Two-port error model.

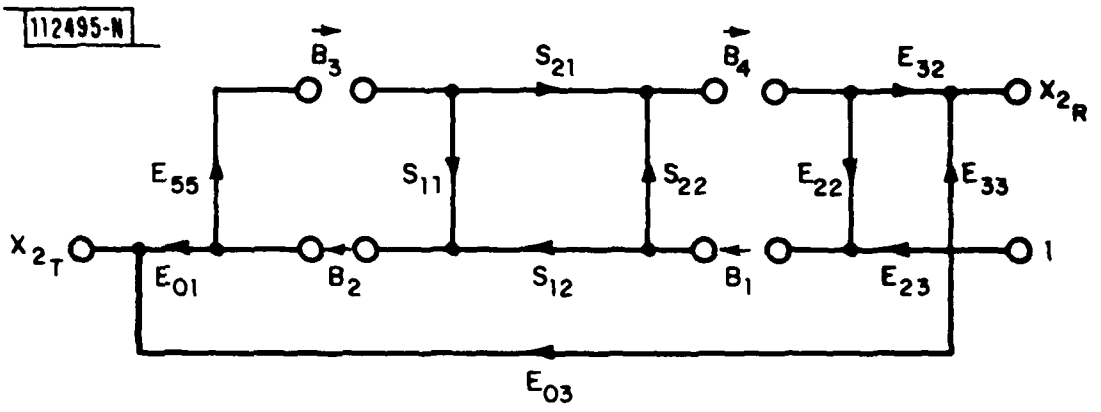

(7) $B_1 = E_{23} + E_{22} B_4$

(8) $B_3 = E_{55} B_2$

(9) $X_{2_R} = E_{33} + E_{32} B_4$

(10) $X_{2_T} = E_{01} B_2 + E_{03}$

(11) $B_2 = S_{11} B_3 + S_{12} B_1$

(12) $B_4 = S_{21} B_3 + S_{22} B_1$

(13) $$S_{11} = \frac{A_4 B_1 - A_3 B_2}{A_1 B_1 - A_3 B_3}$$

(14) $$S_{12} = \frac{A_1 B_2 - A_4 B_3}{A_1 B_1 - A_3 B_3}$$

(15) $$S_{21} = \frac{A_2 B_1 - A_3 B_4}{A_1 B_1 - A_3 B_3}$$

(16) $$S_{22} = \frac{A_1 B_4 - A_2 B_3}{A_1 B_1 - A_3 B_3}$$

Fig. 2B. Two-port error model (continued).

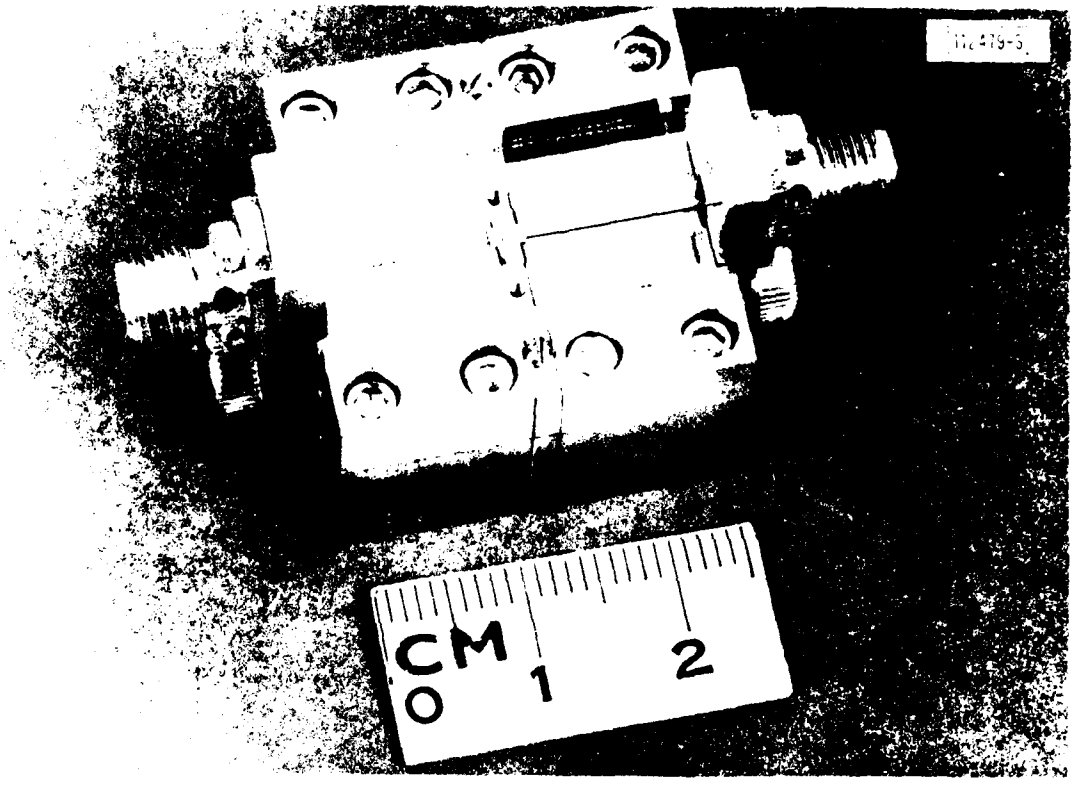

Fig. 3. Microstrip test fixture (50-ohm).

(Fig. 1A) firmly on the microstrip circuit, and independently secures the base of the transistor to the circuit housing to provide both good electrical contact and a good thermal path.

The reflection measurement standards are comprised of 50-ohm microstrip transmission lines of various lengths (Fig. 4), each of which is terminated in a short circuit. The transmission component consists of a 50-ohm microstrip throughline. The design criteria selected to establish accurate calibration with offset shorts constrains the difference in electrical length between the reference short and associated offset shorts to $90° \leq \Delta\Theta \leq 180°$ from which the applicable frequency range is defined for a given set of short circuits. The length of the reference short is identical to that of the input and output 50 ohm circuits in the test holder. For calibration over multi-octave bandwidths, the large number of offset shorts required may introduce biases in the estimates of the error parameters[7] when all are used simultaneously. For narrower bands of an octave or less the biasing effects are eliminated by using just three offset shorts, the minimum number required to solve for the error parameters. This combination of measurement standards and testholder allows testholder contributions to the measurement to be accounted for in the error-correction model.

Both the measurement standards and test-holders utilize .010 inch thick fused-silica substrates solder-mounted on invar carriers. A metallization of 3u gold over 100Å of chrome is applied to the polished substrate. Special coaxial to microstrip launchers (Fig. 5) were designed for this application since commercially available launchers are not compatible with this circuit implementation. The performance of two of these launchers mounted on a half-inch 50-ohm transmission line on a fused silica substrate is shown in Fig. 6. The loss per launcher is determined to be approximately 0.5 dB over the frequency range of interest when the measurement is corrected for substrate loss.

Small signal S-parameter measurements of the transistor installed in the 50-ohm test-circuit are made over the frequency range of 2 - 22 GHz. Typical measurements shown in Fig. 7 are used to calculate other performance parameters[8]

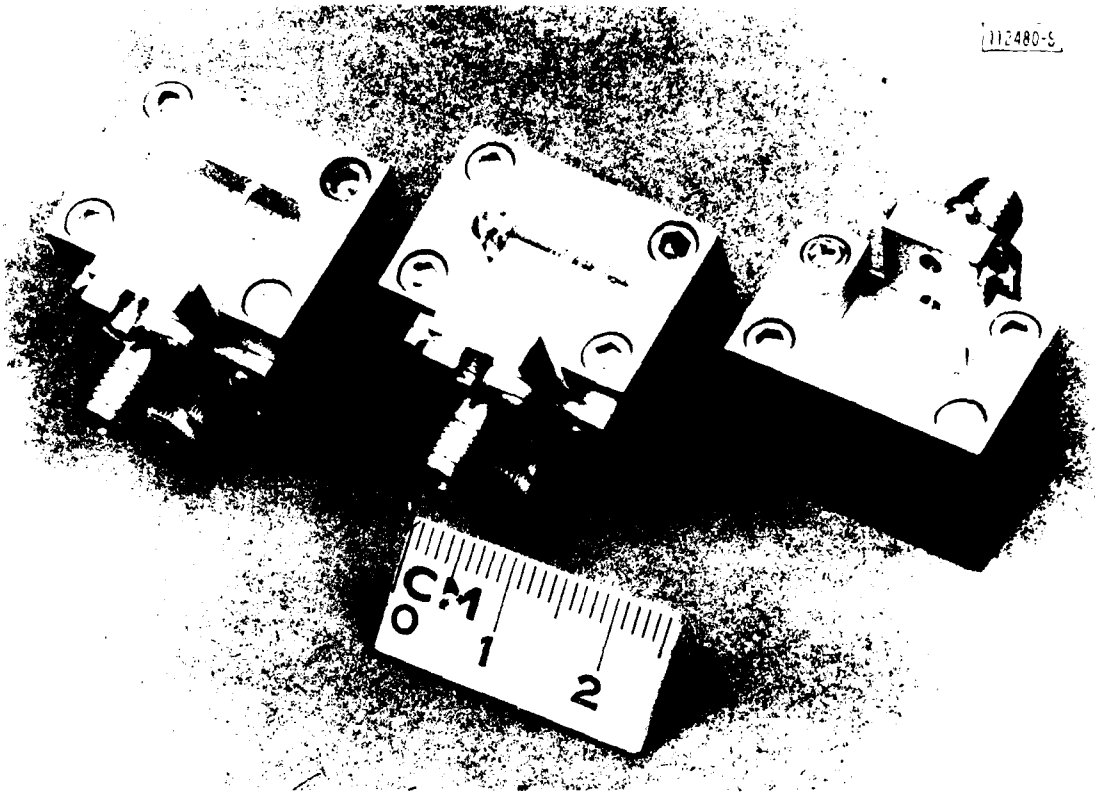

Fig. 4. Microstrip calibration standards: short circuited microstrip lines.

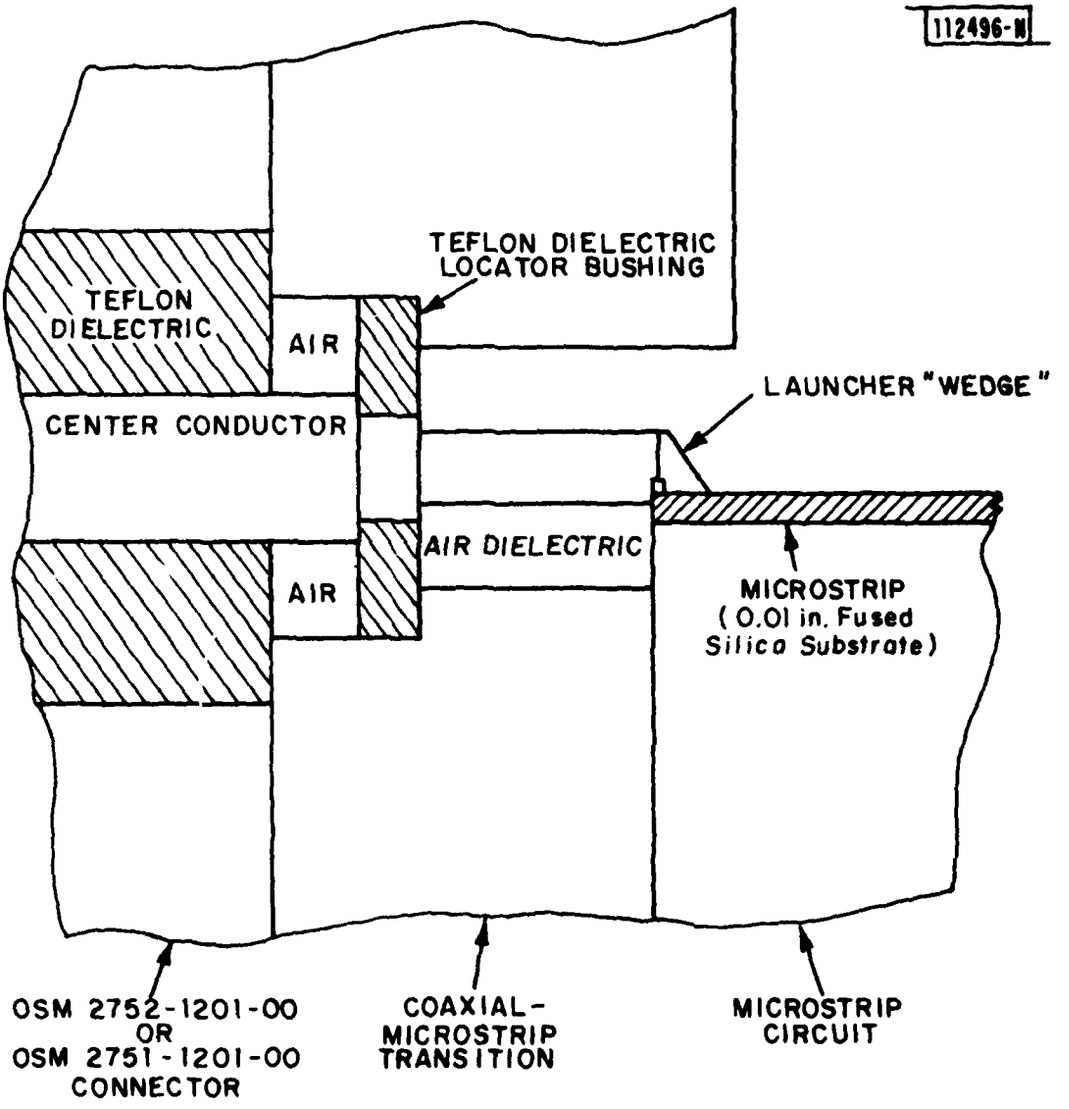

Fig. 5. Coaxial/microstrip launcher.

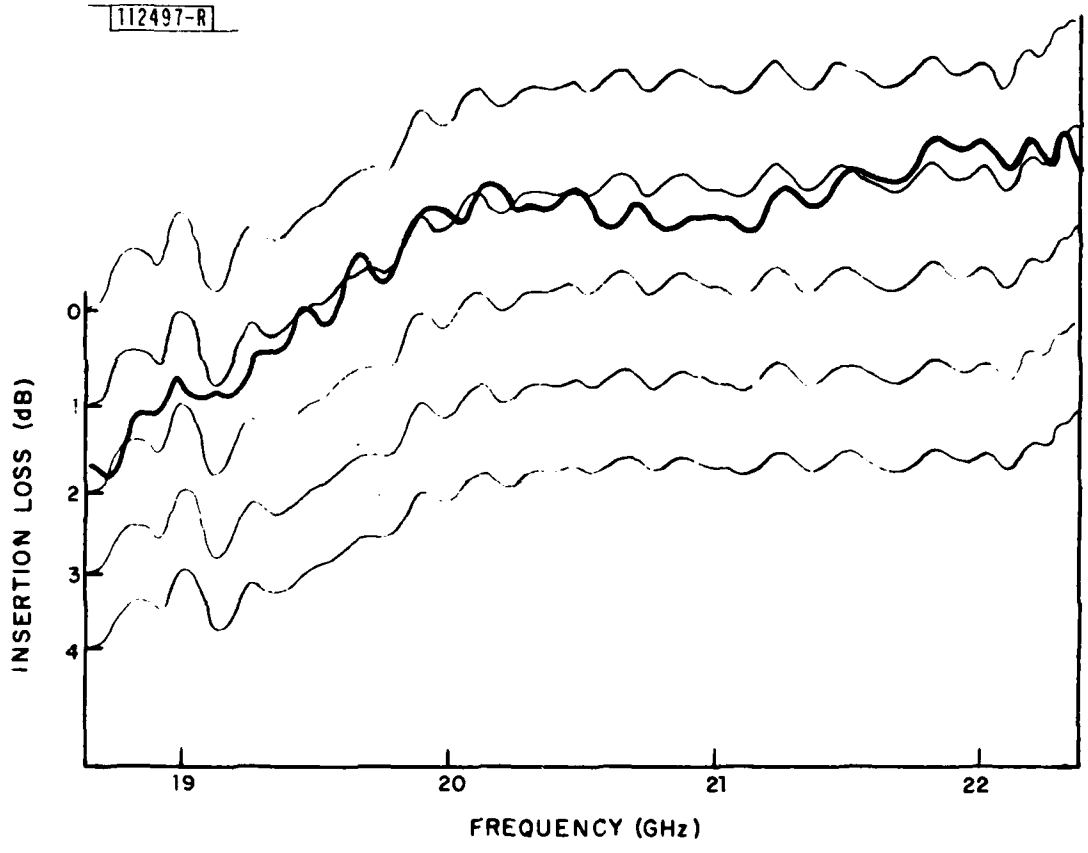

Fig. 6. Coaxial/microstrip launcher performance.

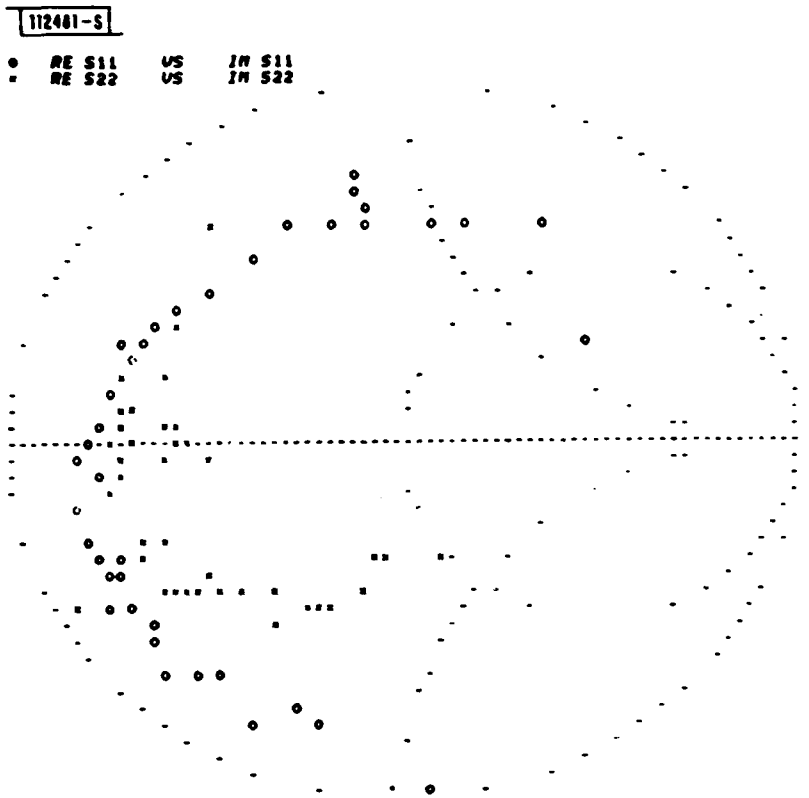

F	MAG S11	DEG S11	MAG S22	DEG S22
2.0000E03	9.7399E-01	-8.5708E01	3.5328E-01	-7.3703E01
2.5000E03	8.1320E-01	-1.0453E02	3.2302E-01	-9.9443E01
3.0000E03	7.8059E-01	-1.0995E02	3.5305E-01	-9.9867E01
3.5000E03	8.7018E-01	-1.1645E02	4.4756E-01	-1.0368E02
4.0000E03	7.9851E-01	-1.2459E02	4.9402E-01	-1.1021E02
4.5000E03	8.3237E-01	-1.2724E02	5.0536E-01	-1.1391E02
5.0000E03	8.0102E-01	-1.3393E02	5.2022E-01	-1.1557E02
5.5000E03	8.3132E-01	-1.3861E02	5.9179E-01	-1.2376E02
6.0000E03	8.0236E-01	-1.4894E02	5.3624E-01	-1.2795E02
6.5000E03	8.3018E-01	-1.4422E02	5.8431E-01	-1.3235E02
7.0000E03	8.7534E-01	-1.4837E02	6.2679E-01	-1.3506E02
7.5000E03	8.1471E-01	-1.5318E02	6.0767E-01	-1.4216E02
8.0000E03	8.0385E-01	-1.5341E02	6.2036E-01	-1.4202E02
8.5000E03	8.0022E-01	-1.5492E02	6.6540E-01	-1.4251E02
9.0000E03	8.3293E-01	-1.5662E02	6.7106E-01	-1.4237E02
9.5000E03	8.4822E-01	-1.6101E02	7.0193E-01	-1.4512E02
1.0000E04	8.5246E-01	-1.6664E02	7.1917E-01	-1.4625E02
1.0500E04	7.6176E-01	-1.6968E02	7.3582E-01	-1.5242E02
1.1000E04	7.8757E-01	-1.7275E02	6.6186E-01	-1.5804E02
1.1500E04	8.1213E-01	-1.7665E02	7.0125E-01	-1.5719E02
1.2000E04	7.9813E-01	1.7936E02	7.0383E-01	-1.5704E02
1.2500E04	7.7699E-01	1.7574E02	7.2089E-01	-1.6596E02
1.3000E04	7.6875E-01	1.7013E02	9.4278E-01	-1.4961E02
1.3500E04	7.3952E-01	1.6408E02	6.8173E-01	-1.7996E02
1.4000E04	7.3583E-01	1.6056E02	6.8197E-01	1.7378E02
1.4500E04	7.5869E-01	1.5927E02	7.1229E-01	1.7218E02
1.5000E04	7.2873E-01	1.5611E02	7.2453E-01	1.7552E02
1.5500E04	7.0922E-01	1.5387E02	7.2713E-01	-1.7909E02
1.6000E04	6.9123E-01	1.4590E02	7.1868E-01	-1.7507E02
1.6500E04	6.5984E-01	1.3800E02	7.2175E-01	1.7382E02
1.7000E04	6.6839E-01	1.2595E02	7.4772E-01	-1.7004E02
1.7500E04	6.5628E-01	1.1620E02	6.7568E-01	1.7904E02
1.8000E04	6.4611E-01	1.0636E02	5.3720E-01	-1.7036E02
1.8500E04	7.6021E-01	9.8563E01	5.8992E-01	-1.7904E02
1.9000E04	7.3059E-01	9.9939E01	5.0384E-01	1.7379E02
1.9500E04	6.2733E-01	9.8647E01	5.9607E-01	-1.7409E02
2.0000E04	6.5757E-01	9.0987E01	5.6918E-01	1.7495E02
2.0500E04	5.9858E-01	8.3206E01	6.8393E-01	1.7608E02
2.1000E04	6.3243E-01	7.5719E01	6.1946E-01	1.6470E02
2.1500E04	7.0393E-01	6.9856E01	6.7044E-01	1.8067E02
2.2000E04	5.5275E-01	3.1056E01	7.9429E-01	1.2929E02

Fig. 7. Small-signal s-parameter measurements for K-band 0.5 W FET.

of interest, including maximum available gain (MAG), maximum stable gain (MSG), and Rollet's Stability factor (K) (see Appendix B). The transducer gain, maximum available gain, and maximum stable gain calculated from the small signal S-parameter measurements of the 0.5 W GaAs MESFET are plotted in Fig. 8 for the frequency range of 2-22 GHz and listed in Table II. The S-parameter measurements made in the 50-ohm microstrip test-fixture in conjunction with the microstrip calibration standards provide characterization at the "packaged transistor" terminals; consequently, the calculated performance parameters are those of the "packaged transistor" only. The reference plane for S-parameters associated with the FET established by the reference microstrip short results in typical lead lengths of two to three thousandths of an inch included in the "packaged transistor", corresponding to the physical distance between the circuit and the transistor required to accommodate the dimensional tolerances associated with these components. Considerable scatter is noted in the calculated gains shown in Fig. 8. This scatter is thought to be primarily the result of parasitics associated with the FET packaging configuration, since similar characterizations of "unpackaged" transistor chips have shown much less scatter. Nevertheless, the visible trend indicates the presence of positive available gain in the frequency range of interest, in addition to the frequency-rolloff characteristic of this transistor. The small signal S-parameters are also used to investigate the stability of the transistor, particularly at low frequencies where the transistor gain is high.

While the small-signal S-parameters are useful for the design of linear amplifiers, they are of less usefulness in designing power amplifiers. Power amplifier design is greatly enhanced by appropriate large signal characterizations since the transistor typically exhibits non-linear behavior under large-signal conditions. In addition, the large-signal operating conditions established by conventional one signal measurement of S-parameters associated with the transistor output (i.e., S_{22} or S_{12}) do not correspond to actual amplifier large-signal operating conditions since the signal conditions at the transistor input are quite different when the transistor is excited from the output instead of the input. Consequently, additional techniques are required to obtain a valid large-signal S-parameter description of the transistor.

TABLE II

SMALL-SIGNAL S-PARAMETERS AND CALCULATED PERFORMANCE PARAMETERS
(MAG, MSG, K) FOR K-BAND 0.5 FET.

F	MAG S11	DEG S11	MAG S12	DEG S12	MAG S21	DEG S21	MAG S22	DEG S22
2.0000E03	9.7399E-01	-8.5705E01	2.5046E-02	3.0549E01	6.0490E00	1.1130E02	3.5320E-01	-7.3703E01
2.5000E03	8.1320E-01	-1.8453E02	2.7791E-02	1.0066E01	4.7997E00	9.4661E01	3.2302E-01	-9.9443E01
3.0000E03	7.8059E-01	-1.8995E02	1.9528E-02	7.3071E00	2.9831E00	8.3870E01	3.5305E-01	-9.9867E01
3.5000E03	8.7018E-01	-1.1645E02	2.1133E-02	8.5243E00	2.6949E00	8.0405E01	4.4756E-01	-1.0360E02
4.0000E03	7.9851E-01	-1.2459E02	3.3843E-02	1.0090E00	2.6806E00	6.9329E01	4.9482E-01	-1.1021E02
4.5000E03	8.3237E-01	-1.2724E02	1.8933E-02	-2.7670E00	1.6151E00	6.7598E01	5.8536E-01	-1.1391E02
5.0000E03	8.8102E-01	-1.3393E02	2.4487E-02	2.4953E00	2.3513E00	7.0733E01	5.2822E-01	-1.1557E02
5.5000E03	8.3132E-01	-1.3861E02	3.3356E-02	5.0000E00	2.0735E00	5.2837E01	5.9179E-01	-1.2376E02
6.0000E03	8.8236E-01	-1.4894E02	2.8942E-02	-1.5425E01	1.4010E00	3.9245E01	5.3624E-01	-1.2795E02
6.5000E03	8.3010E-01	-1.4422E02	2.0671E-02	1.5903E01	1.1177E00	4.7495E01	5.0431E-01	-1.3235E02
7.0000E03	8.7534E-01	-1.4837E02	2.0985E-02	-8.3516E00	1.4014E00	4.9174E01	6.2679E-01	-1.3586E02
7.5000E03	8.1471E-01	-1.5316E02	4.2094E-02	-1.3167E01	1.4417E00	2.0670E01	6.8767E-01	-1.4216E02
8.0000E03	8.0385E-01	-1.5341E02	2.8213E-02	-3.1692E01	9.7490E-01	2.5659E01	6.2836E-01	-1.4202E02
8.5000E03	8.0022E-01	-1.5492E02	2.1459E-02	-2.0585E01	7.8095E-01	2.9793E01	6.6548E-01	-1.4251E02
9.0000E03	8.3293E-01	-1.5662E02	2.1413E-02	-2.3047E01	7.2789E-01	2.3470E01	6.7186E-01	-1.4237E02
9.5000E03	8.4822E-01	-1.6181E02	2.2255E-02	-3.2841E01	7.3310E-01	2.0836E01	7.8193E-01	-1.4512E02
1.0000E04	8.5246E-01	-1.6664E02	2.3967E-02	-3.6305E01	9.3815E-01	3.1416E01	7.1917E-01	-1.4625E02
1.0500E04	7.6176E-01	-1.6968E02	3.5312E-02	-3.2310E01	9.4647E-01	1.6859E01	7.3582E-01	-1.5242E02
1.1000E04	7.8757E-01	-1.7275E02	3.1877E-02	-3.6830E01	7.4484E-01	4.2733E-01	6.6106E-01	-1.5504E02
1.1500E04	8.1213E-01	-1.7665E02	2.7314E-02	-4.5403E01	6.4921E-01	1.0660E01	7.8125E-01	-1.5719E02
1.2000E04	7.9813E-01	1.7936E02	2.7804E-02	-3.9687E01	1.0121E00	-9.0474E00	7.0383E-01	-1.5784E02
1.2500E04	7.7699E-01	1.7574E02	3.7843E-02	-5.7867E01	1.0418E00	-1.3529E01	7.2889E-01	-1.6596E02
1.3000E04	7.6875E-01	1.7813E02	3.5307E-02	-5.9684E01	7.7339E-01	-1.0786E01	9.4278E-01	-1.4961E02
1.3500E04	7.3952E-01	1.6408E02	3.1187E-02	-6.6919E01	7.7032E-01	-4.2238E01	6.8173E-01	-1.7996E02
1.4000E04	7.3503E-01	1.6056E02	2.5706E-02	-6.2367E01	5.0301E-01	3.1638E01	6.8197E-01	-1.7378E02
1.4500E04	7.5869E-01	1.5927E02	2.4565E-02	-5.7622E01	5.8159E-01	-2.8097E01	7.1229E-01	-1.7218E02
1.5000E04	7.2873E-01	1.5611E02	2.6788E-02	-5.4021E01	5.2863E-01	-3.5210E01	7.2453E-01	-1.7552E02
1.5500E04	7.0922E-01	1.5307E02	2.6867E-02	-5.7122E01	4.7279E-01	-3.8450E01	7.2713E-01	-1.7989E02
1.6000E04	6.9123E-01	1.4590E02	2.5373E-02	-5.2037E01	5.3420E-01	-3.3860E01	7.1060E-01	-1.7507E02
1.6500E04	6.5984E-01	1.3800E02	2.7073E-02	-5.5271E01	5.4440E-01	-3.6805E01	7.2175E-01	-1.7382E02
1.7000E04	6.6039E-01	1.2595E02	3.3618E-02	-5.3139E01	6.3381E-01	-3.9827E01	7.4772E-01	-1.7804E02
1.7500E04	6.5620E-01	1.1620E02	3.4802E-02	-5.8686E01	1.0724E00	-3.4430E01	6.7560E-01	-1.7904E02
1.8000E04	6.4611E-01	1.0636E02	3.1829E-02	-6.3845E01	1.0357E00	-6.2693E01	5.3720E-01	-1.7036E02
1.8500E04	7.6021E-01	9.8563E01	4.5595E-02	-8.7124E01	6.6448E-01	-7.9859E01	5.5992E-01	-1.7984E02
1.9000E04	7.3089E-01	9.9939E01	3.8178E-02	-1.0661E02	4.9710E-01	-8.0224E01	5.0384E-01	-1.7379E02
1.9500E04	6.2733E-01	9.0647E01	2.6057E-02	-7.9525E01	4.0366E-01	-6.9835E01	5.9607E-01	-1.7489E02
2.0000E04	6.5757E-01	9.0957E01	2.5065E-02	-5.8570E01	5.5362E-01	-6.9530E01	5.6918E-01	-1.7495E02
2.0500E04	5.9058E-01	8.3206E01	3.8074E-02	-6.3601E01	5.9339E-01	-6.9946E01	6.8393E-01	-1.7608E02
2.1000E04	6.3243E-01	7.5719E01	4.7210E-02	-7.7247E01	7.2967E-01	-8.0635E01	6.1946E-01	-1.6478E02
2.1500E04	7.0393E-01	5.9856E01	5.4809E-02	-8.2641E01	7.2663E-01	-9.7282E01	6.7044E-01	-1.5857E02
2.2000E04	5.5275E-01	3.1856E01	6.0622E-02	-8.0102E01	9.4128E-01	-9.4902E01	7.9429E-01	-1.2929E02

F: Frequency in MHz

TABLE II (Continued)

F	RE ZM1	IM ZM1	RE ZM2	IM ZM2	DB TG	DB MG	DBMAG RF	DB ISF	ISF
2.0000E03	0.0000E00	6.1031E01	-1.7477E-14	-9.2477E00	1.5635E01	3.7362E01	2.3693E01	-1.3668E01	4.2978E-02
2.5000E03	1.9107E00	3.6984E01	5.9777E00	2.5768E01	1.3624E01	2.1171E01	2.2373E01	1.6431E-01	1.0386E00
3.0000E03	7.9728E00	3.3518E01	2.6308E01	2.6048E01	9.4932E00	1.4467E01	2.1840E01	4.5064E00	2.8225E00
3.5000E03	2.8369E00	3.0865E01	1.3112E01	2.9209E01	6.6109E00	1.7085E01	2.1056E01	1.6074E00	1.4479E00
4.0000E03	3.9475E00	2.4254E01	1.0789E01	2.4689E01	6.5646E00	1.5512E01	1.8988E01	1.2636E00	1.3377E00
4.5000E03	5.0018E00	2.3987E01	1.7870E01	2.5589E01	4.1642E00	1.0940E01	1.9310E01	5.4585E00	3.5079E00
5.0000E03	8.5254E-01	2.0436E01	3.7453E00	2.5056E01	7.4261E00	1.8404E01	1.9038E01	2.3253E-01	1.0550E00
5.5000E03	1.6158E00	1.7577E01	4.2337E00	2.1623E01	6.3341E00	1.5938E01	1.7935E01	4.4395E-01	1.1076E00
6.0000E03	5.4049E00	1.6594E01	1.4838E01	1.8495E01	2.9288E00	9.2188E00	1.6849E01	4.7475E00	2.9836E00
6.5000E03	4.5566E00	1.5494E01	1.3022E01	1.8625E01	9.6676E-01	8.2107E00	1.7338E01	6.1734E00	4.1433E00
7.0000E03	2.4608E00	1.3614E01	8.1972E00	1.7336E01	2.9312E00	1.2582E01	1.8247E01	2.9626E00	1.9701E00
7.5000E03	2.2181E00	9.0759E00	3.9300E00	1.2715E01	3.1774E00	1.2732E01	1.5347E01	7.4378E-01	1.1868E00
8.0000E03	5.2321E00	1.0856E01	1.1453E01	1.3968E01	2.2011E-01	6.6491E00	1.5305E01	5.8831E00	3.8046E00
8.5000E03	5.3390E00	1.0486E01	1.0006E01	1.5190E01	2.1476E00	5.0981E00	1.5618E01	7.5358E00	5.6700E00
9.0000E03	4.3752E00	9.7567E00	9.8048E00	1.5002E01	2.7587E00	5.2355E00	1.5314E01	7.1098E00	5.1402E00
9.5000E03	4.0639E00	7.6904E00	8.5174E00	1.3723E01	2.6967E00	5.8528E00	1.5177E01	6.3731E00	4.3382E00
1.0000E04	3.1826E00	5.8758E00	6.7178E00	1.3003E01	6.2895E-01	8.9121E00	1.5809E01	4.1303E00	2.5932E00
1.0500E04	5.3650E00	3.1150E00	6.2479E00	1.8458E01	4.7787E-01	7.3622E00	1.4282E01	4.8852E00	2.5617E00
1.1000E04	5.5019E00	2.3222E00	9.6378E00	8.9752E00	2.5587E00	4.3760E00	1.3686E01	6.3588E00	4.3239E00
1.1500E04	4.7216E00	8.0793E-01	8.1432E00	8.5368E00	3.7523E00	4.1639E00	1.3760E01	6.6378E00	4.6109E00
1.2000E04	4.6388E00	-1.2220E00	7.2384E00	8.2622E00	1.8461E-01	8.8652E00	1.5611E01	4.6681E00	2.9296E00
1.2500E04	4.5331E00	-3.3233E00	-5.7166E00	8.8688E00	3.5558E-01	8.6863E00	1.4398E01	-3.8738E00	2.8291E00
1.3000E04	8.8888E00	-1.8677E01	7.2603E-16	1.1871E01	2.2320E00	1.3474E01	1.3405E01	6.8449E-02	9.8436E-01
1.3500E04	7.6392E00	-7.8647E00	9.4312E00	-1.3683E00	2.2666E00	3.8782E00	1.3927E01	7.8888E00	5.1059E00
1.4000E04	7.6888E00	-8.8944E00	9.1787E00	-3.3379E00	5.9684E00	2.3861E-01	1.2982E01	9.6736E00	9.2761E00
1.4500E04	6.6914E00	-9.5673E00	7.9266E00	-4.8650E00	-4.7877E00	2.2806E00	1.3743E01	8.4741E00	7.8374E00
1.5000E04	7.8185E00	-1.0986E01	7.6823E00	-2.5536E00	5.5369E00	-1.1392E00	1.2966E01	8.8356E00	7.6482E00
1.5500E04	8.6364E00	-1.2245E01	7.5627E00	-5.7169E-01	6.5065E00	-7.1330E-02	1.2454E01	9.5298E00	8.9723E00
1.6000E04	9.5745E00	-1.5436E01	8.0935E00	1.5886E00	5.4459E00	5.6331E-01	1.3233E01	9.6723E00	9.2733E00
1.6500E04	1.1241E01	-1.9189E01	7.7336E00	2.1547E00	5.2816E00	5.3405E-01	1.3834E01	9.5832E00	8.9191E00
1.7000E04	1.1768E01	-2.5588E01	6.6209E00	-3.6802E00	-3.9608E00	2.3643E00	1.2755E01	7.4165E00	5.5163E00
1.7500E04	1.0624E01	-3.1819E01	7.0298E00	-1.1690E00	6.0731E-01	6.5629E00	1.2916E01	3.5694E00	2.2748E00
1.8000E04	1.4748E01	-3.7437E01	1.2736E01	-2.8411E00	-3.0473E-01	4.5072E00	1.2297E01	4.8988E00	3.0889E00
1.8500E04	1.1679E01	-4.3886E01	1.3651E01	-2.1562E00	-3.5504E00	-1.8987E00	1.1636E01	6.7754E00	4.7593E00
1.9000E04	1.3428E01	-4.8781E01	1.7804E01	1.4932E00	-6.0711E00	-1.5507E00	1.2168E01	1.0716E01	1.1792E01
1.9500E04	1.9195E01	-3.9947E01	1.2492E01	-1.6052E00	-6.3092E00	-2.1961E00	1.2606E01	1.1877E01	1.5485E01
2.0000E04	1.6965E01	-4.0313E01	1.3256E01	-2.4816E00	-5.1357E00	-8.8384E-01	1.3441E01	1.1321E01	1.3555E01
2.0500E04	2.6038E01	-5.8098E01	1.1656E01	-2.8748E00	-4.5331E00	-5.4721E-01	1.1927E01	9.4779E00	8.8674E00
2.1000E04	2.6547E01	-5.9652E01	1.8896E01	-7.3933E00	-2.7375E00	1.8353E00	1.1890E01	7.8867E00	5.1129E00
2.1500E04	2.8476E01	-8.4391E01	8.4466E00	-1.3777E01	-2.7738E00	3.4264E00	1.1218E01	4.9800E00	3.0983E00
2.2000E04	8.2518E01	-1.1181E02	5.1402E00	-2.3096E01	-5.2635E-01	6.3823E00	1.2693E01	3.6039E00	2.2929E00

ZM1: Conjugate-Match Generator Impedance
ZM2: Conjugate-Match Load Impedance
F: Frequency in MHz
TG: Tranducer Gain
MG: Maximum Available Gain
MAG RF: Maximum Stable Gain
ISF: Rollett's Invariant Stability Factor
(See Appendix II)

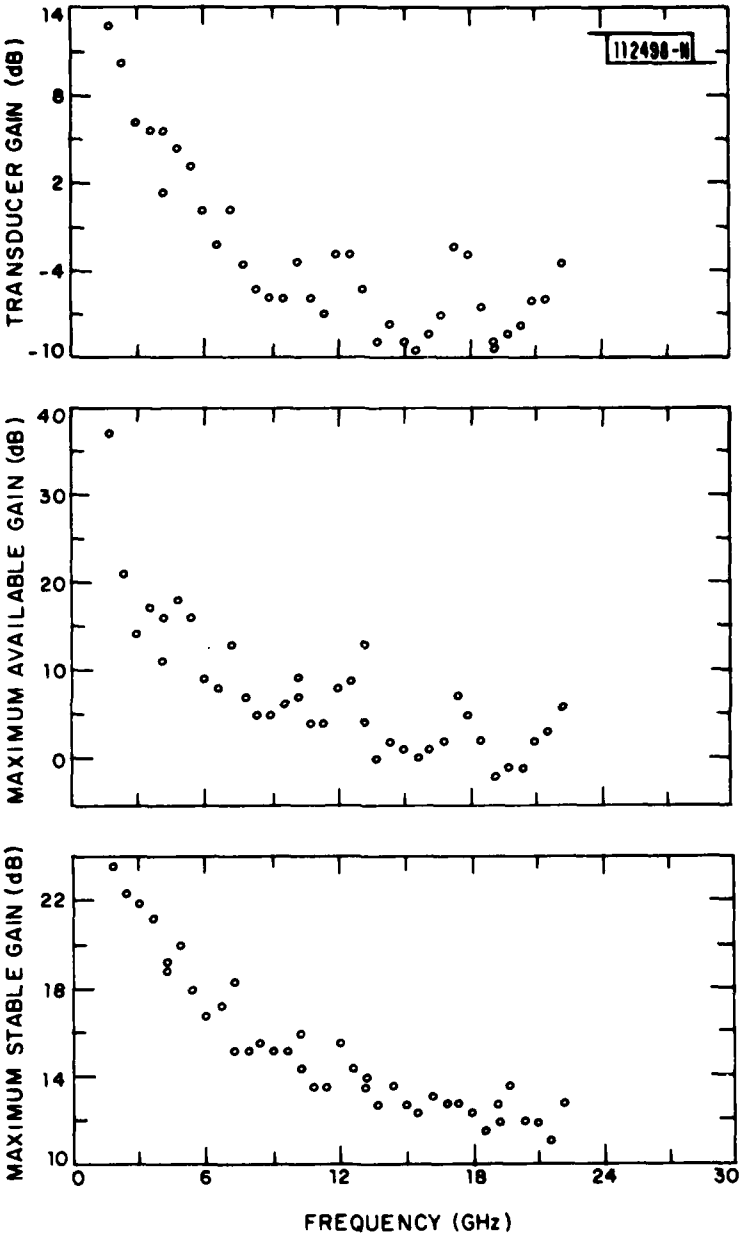

Fig. 8. Performance parameters calculated from small-signal s-parameter measurements of K-band 0.5 W FET.

A novel measurement technique for characterizing active two-port networks has been reported by Mazumder and Van Der Puije[9]. This technique is referred to as the two-signal method of measuring large-signal S-parameters. The scattering-parameter description of a two-port network is shown in Fig. 9. The complex wave variables are related to the scattering coefficients by Equations 20 and 21. These wave variables may be defined in terms of voltages and currents as given in expressions (22) through (25)[10]. The quantities a_1 and a_2 are the independent variables, corresponding to the waves incident upon port 1 and port 2 respectively; b_1 and b_2 are the dependent variables, corresponding to the wave exiting these ports. The two-signal measurement method requires excitation of both ports of the network simultaneously at identical frequency. The notation adopted provides an adequate description for representing this interaction (i.e., a_1 and a_2 represent the two excitations).

The instrument configuration required to provide this measurement capability is shown in the Fig. 10. The signal from the synthesized signal source is amplified by a traveling-wave-tube amplifier and split equally to provide the two excitations required for testing. Each arm of the test configuration includes a variable attenuator to provide absolute and relative amplitude control of each signal. Relative phase between the two signals is controlled by the phase shifter. The couplers provide access to the wave quantities to be measured, and circulators permit direct measurement of power while also isolating one arm of the test system from the other. A switching network permits selection of the desired quantities for measurement by the network analyzer. The test system is controlled with an HP 9845B desktop computing system, which together with appropriate software and measurement standards provides complete two-port error-correction of measured data as described earlier. Conventional one-signal automated S-parameter measurements are made by replacing the power splitter in this configuration by a programmable switch.

It is helpful to consider the interaction between the two signals incident upon the two ports of the network by examining the equations describing the two-port S-parameters.

112499-N

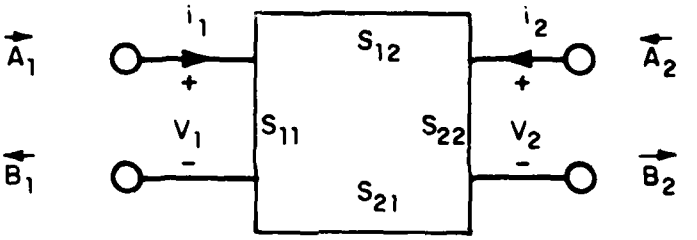

$$(20)\quad \vec{B}_1 = S_{11}\vec{A}_1 + S_{12}\vec{A}_2$$

$$(21)\quad \vec{B}_2 = S_{21}\vec{A}_1 + S_{22}\vec{A}_2$$

$$(22)\quad A_1 = \frac{1}{2\sqrt{Z_0}}(v_1 + Z_0\, i_1)$$

$$(23)\quad A_2 = \frac{1}{2\sqrt{Z_0}}(v_2 + Z_0\, i_2)$$

$$(24)\quad B_1 = \frac{1}{2\sqrt{Z_0}}(v_1 - Z_0\, i_1)$$

$$(25)\quad B_2 = \frac{1}{2\sqrt{Z_0}}(v_2 - Z_0\, i_2)$$

Fig. 9. Scattering-parameter description for two-port network.

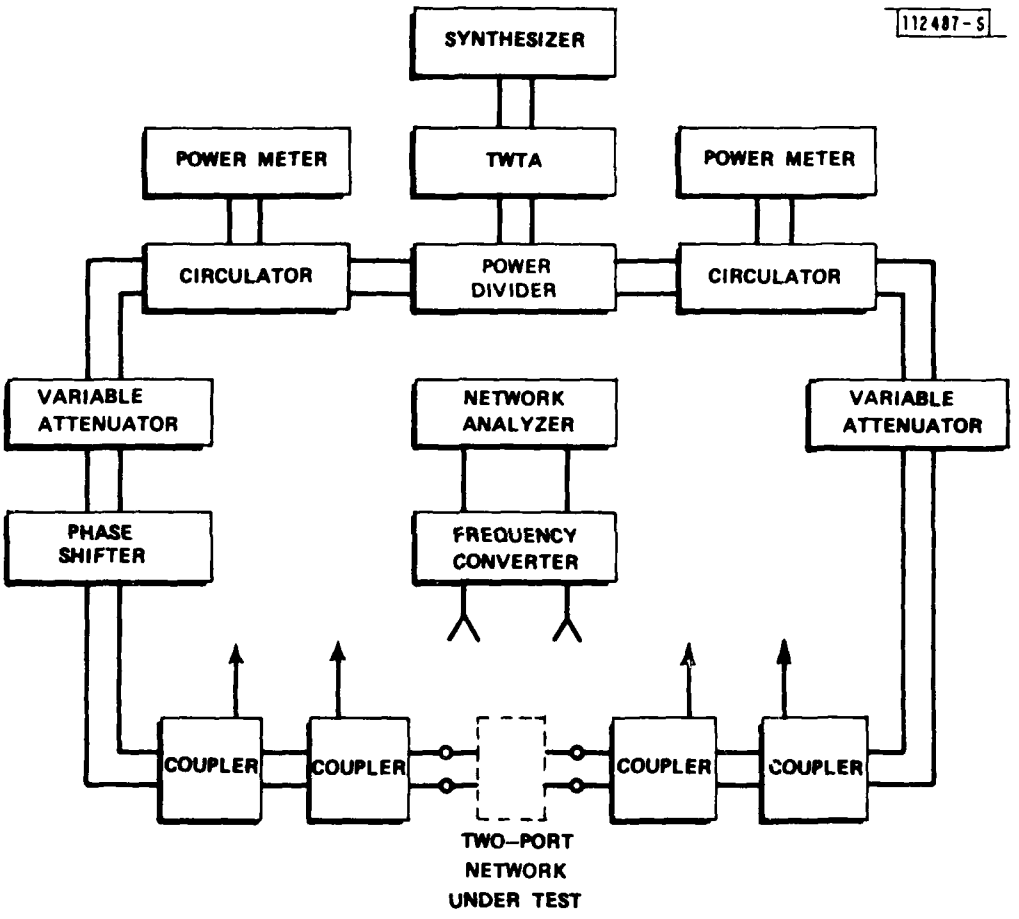

Fig. 10. Test configuration for two-signal measurement.

$$(20)\quad b_1 = S_{11}a_1 + S_{12}a_2$$

$$(21)\quad b_2 = S_{21}a_1 + S_{22}a_2$$

These equations may be rearranged to obtain four expressions relating ratios of complex wave variables--that is, reflection and transmission coefficients--to scattering coefficients (S_{ij}).

$$(26)\quad b_1/a_1 = S_{11} + S_{12}(a_2/a_1)$$

$$(27)\quad b_1/a_2 = S_{11}(a_1/a_2) + S_{12}$$

$$(28)\quad b_2/a_1 = S_{21} + S_{22}(a_2/a_1)$$

$$(29)\quad b_2/a_2 = S_{21}(a_1/a_2) + S_{22}$$

These ratios are the quantities which are measured, and since the independent variables are known (a_1 and a_2 are set to the desired large signal amplitudes), the S-parameters can be determined by allowing $\measuredangle (a_2/a_1)$ to vary through 360°. Furthermore, if $|a_1| = |a_2|$ = constant, the extraction of S-parameter data is simplified.

The interaction between the two signals can be illustrated graphically as shown in Fig. 11. Each of the ratios of complex wave variables is plotted in its respective complex plane. The circular loci shown for each of the complex ratios are generated by allowing $\measuredangle a_2/a_1$ to vary through 360°. From equations (26) through (29), each of these loci may be resolved into its respective components. For example, the b_2/a_2 ratio is resolved into S_{22} and S_{21} (a_2/a_1).

It should be noted that the large-signal S-parameters determined in this fashion are valid only at the signal levels under which the measurement is made; measurement at other signal conditions may yield a different set of S-parameters. To distinguish between conventional S-parameters and the large-signal parameters obtained by injection of two signals, a designation of P-parameters is assigned to the latter[11].

A unique set of P-parameters is then determined for discrete power levels. Characterization of the transistor is then accomplished at a power level corresponding to that desired in a particular amplifier design.

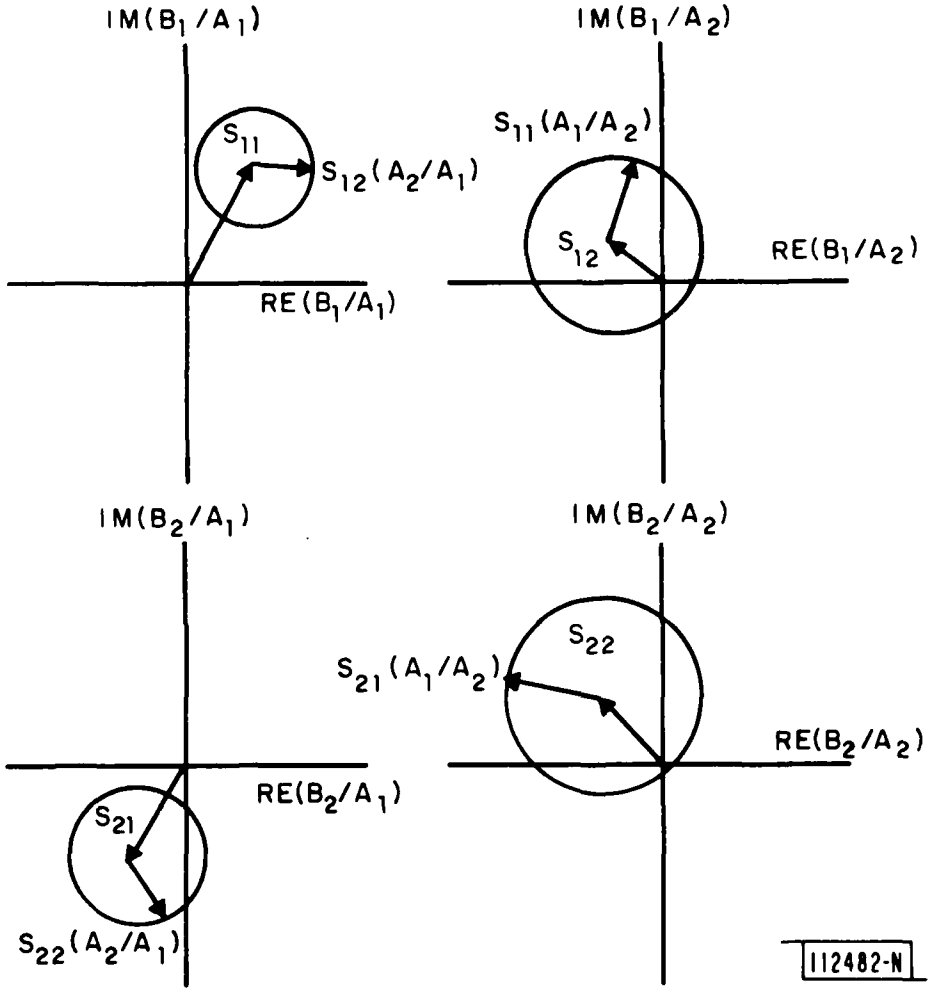

Fig. 11. Reflection/transmission coefficients generated by two-signal measurements.

Extraction of the P-parameter information is illustrated in Fig. 12. Coordinates (h,k) are assigned to C_1, the center of the locus; (X_1, Y_1) is assigned to P_1 (the first measured b_2/a_2 ratio in this example), and so on to (X_n, Y_n) for P_N. For a circular locus an equation for the radius of the circle at P_1 can be written; in similar fashion an equation for the radius at each P_N can be written, yielding equation set (31).

$$(31)\quad \left\{\begin{array}{c} (X_1 - H)^2 + (Y_1 - K)^2 = R^2 \\ (X_2 - H)^2 + (Y_2 - K)^2 = R^2 \\ \vdots \qquad\qquad \vdots \qquad\qquad \vdots \\ (X_N - H)^2 + (Y_N - K)^2 = R^2 \end{array}\right\}$$

Expanding the terms in parentheses and rearranging yields equation set (32).

$$(32)\quad \left\{\begin{array}{c} -(H^2 + K^2 - R^2) + 2X_1H + 2Y_1K = X_1^2 + Y_1^2 \\ -(H^2 + K^2 - R^2) + 2X_2H + 2Y_2K = X_2^2 + Y_2^2 \\ \vdots \qquad\qquad\qquad \vdots \qquad\qquad\qquad \vdots \\ -(H^2 + K^2 - R^2) + 2X_NH + 2Y_NK = X_N^2 + Y_N^2 \end{array}\right\}$$

These equations are solved using the matrix notation of equation (33) from which the desired P-parameter information is obtained.

$$(33)\quad \begin{bmatrix} 2X_1 & 2Y_1 & -1 \\ 2X_2 & 2Y_2 & -1 \\ \vdots & \vdots & \vdots \\ 2X_N & 2Y_N & -1 \end{bmatrix} \begin{bmatrix} H \\ K \\ \vdots \\ H^2 + K^2 - R^2 \end{bmatrix} = \begin{bmatrix} X_1^2 + Y_1^2 \\ X_2^2 + Y_2^2 \\ \vdots \\ X_N^2 + Y_N^2 \end{bmatrix}$$

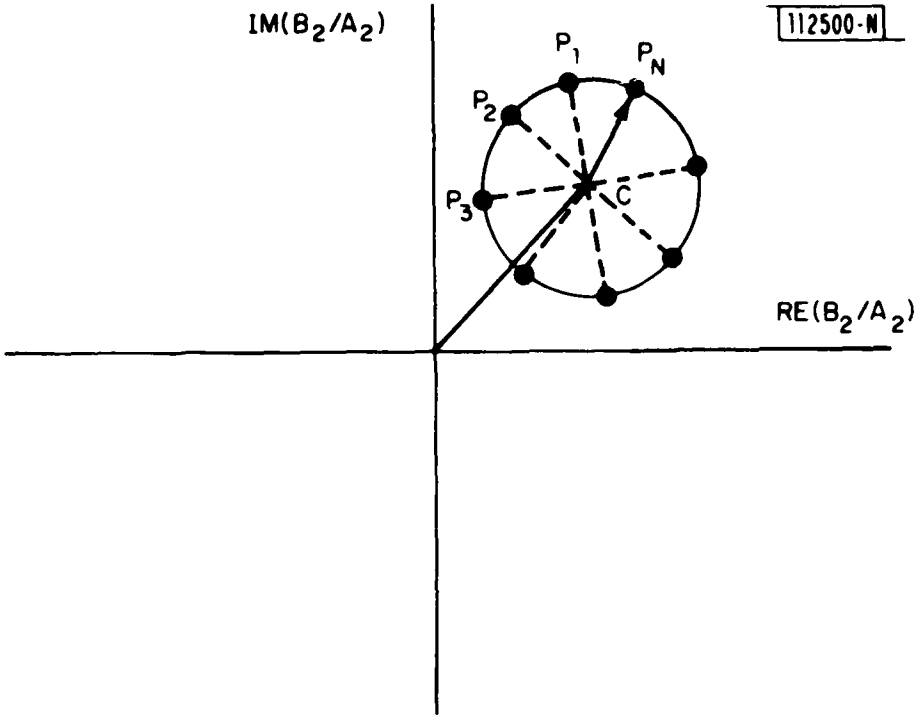

FOR $|A_2| = |A_1| = \text{CONSTANT}$,

$$B_2/A_2 = S_{21}\frac{A_1}{A_2} + S_{22} \tag{29}$$

$$= S_{21} + S_{22}$$

30
$C \rightarrow C\,(H,K)$
$P_1 \rightarrow P_1\,(X_1, Y_1)$
$P_2 \rightarrow P_2\,(X_2, Y_2)$
•
•
•
$P_N \rightarrow P_N\,(X_N, Y_N)$

Fig. 12. Notation for extraction of p-parameter information.

Let $[A] = \begin{bmatrix} 2X_1 & 2Y_1 & -1 \\ 2X_2 & 2Y_2 & -1 \\ \vdots & \vdots & \vdots \\ 2X_N & 2Y_N & -1 \end{bmatrix}$, $[X] = \begin{bmatrix} H \\ K \\ \vdots \\ H^2 + K^2 - R^2 \end{bmatrix}$

$$[B] = \begin{bmatrix} X_1^2 + Y_1^2 \\ X_2^2 + Y_2^2 \\ \vdots \\ X_N^2 + Y_N^2 \end{bmatrix}$$

(34) $[A]\,[X] = [B]$

(35) $[X] = ([A^T]\,[A])^{-1}\,[A^T]\,[B]$

(36) $|P_{22}| = \sqrt{H^2 + K^2}$

(37) $\measuredangle P_{22} = \text{TAN}^{-1}\,(K/H)$

(38) $|P_{21}| = \sqrt{(H^2 + K^2) - (H^2 + K^2 - R^2)} = R$

Other P-parameters are determined in a similar fashion to that described above. The two-signal measurement technique is novel in the sense that no tuners are required to obtain a large-signal description of the transistor. Fixed tuned circuits are used which enhances the repeatability and accuracy of measurements.

The two-signal implementation can also provide additional measurement flexibility. It can function essentially as an electronic tuner since both amplitude and relative phase control of the signal injected at the output port are provided by this configuration. As such it is a lossless tuner. It is also capable of establishing output reflection-coefficients greater

than unity provided additional signal power is still available when the input port of the network under test is driven at the desired signal level.

The procedure for obtaining a large-signal description of the transistor is summarized in Fig. 13. The transistor is first inserted in a test circuit which provides a 50-ohm environment at its input and output ports. A conventional one-signal measurement is made at the transistor input port at the desired signal level. The "large-signal S_{11}" which is determined in this fashion is used to determine the actual power input to the transistor; the power input is then readjusted to correct for the input mismatch. This procedure is iterated until the actual power input to the transistor is sufficiently close to the desired level.

The "large-signal S_{11}" corresponding to the desired power input level thus obtained is used to design an input matching network (IMN). This network provides an input termination which closely approximates that needed for actual amplifier operation at the signal level which was selected. This matching network is installed in the test-holder (replacing the 50Ω input circuit), and the two-signal measurement technique is used to measure P_{11} as a function of frequency and to ensure properly matched conditions at the transistor input port. The two-signal measurement method is then made at the transistor output port to obtain P_{22} from which the output matching network (OMN) is designed. The output matching network designed on this basis (conjugate match for P_{22}) provides maximum gain at the signal level at which the transistor was characterized. This procedure or any part of it is iterated as necessary, depending on the performance achieved.

Typical large-signal characterizations of the .5 watt K-Band GaAs MESFETs developed in this program are shown in Figs. 14 and 15. Conventional one-signal measurements of the transistor installed in the 50-ohm holder described previously show that most of the power incident on the transistor is reflected.

Figure 14 illustrates the result of a two-signal measurement made at large-signal conditions to determine the input impedance match for a FET with a partial-matching network installed in the input port of the FET test-circuit.

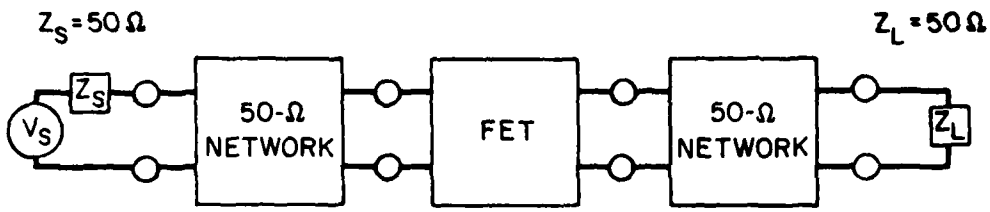

I CONVENTIONAL ONE-SIGNAL S-PARAMETER MEASUREMENT

- MEASURE S_{11} UNDER LARGE-SIGNAL CONDITIONS
- ITERATE TO ESTABLISH DESIRED INPUT LEVEL
- DESIGN MATCHING NETWORK (IMN) FOR FET INPUT

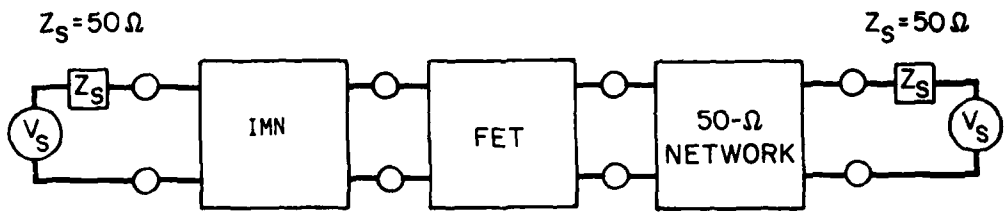

II TWO-SIGNAL S-PARAMETER MEASUREMENT

- INSTALL IMN AND MEASURE S_{11} TO DETERMINE INPUT MATCH
- MEASURE S_{22} UNDER LARGE-SIGNAL CONDITIONS
- DESIGN OUTPUT MATCHING NETWORK

112488-S

Fig. 13. Large-signal FET characterization and circuit design procedure.

FREQUENCY (MHz)	MAG P11	ARG P11 (deg)	MAG P12	REVERSE GAIN (dB)	INPUT RETURN LOSS (dB)
20000	.81	149.42	.203	-13.85	-1.82
20100	.73	151.06	.216	-13.30	-2.68
20200	.78	154.04	.211	-13.53	-2.17
20300	.74	154.95	.217	-13.29	-2.61
20400	.72	157.76	.243	-12.29	-2.86
20500	.72	161.44	.254	-11.90	-2.81
20600	.71	163.26	.258	-11.77	-2.98
20700	.59	162.60	.235	-12.57	-4.57
20800	.57	163.99	.257	-11.79	-4.86
20900	.58	168.90	.287	-10.83	-4.70
21000	.52	174.94	.327	-9.71	-5.62

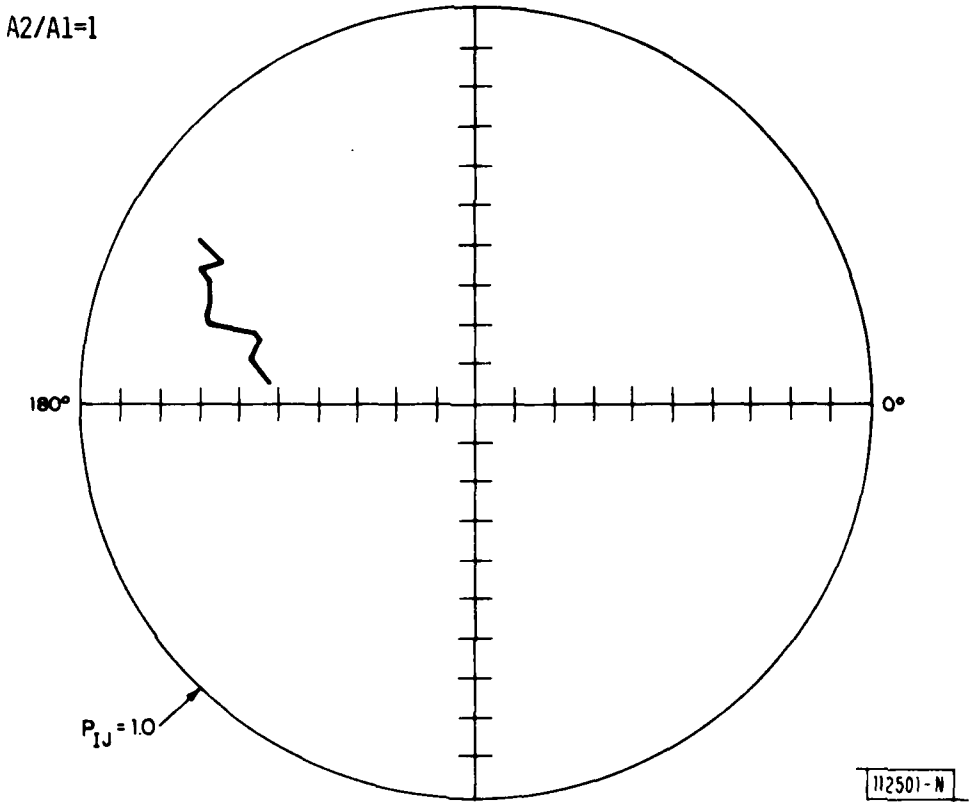

Fig. 14. P-parameter measurements: K-band 0.5 W FET, P_{11} (partial input matching network installed).

This network is seen to provide an impedance match which improves as frequency increases; the best match, $P_{11} = .52/\underline{174.9}°$, occurs at 21 GHz, corresponding to an actual power input to the transistor of 22.6 dBmW for the measurement conditions (generator power = +24 dBmW). Figure 15A shows the measured P_{22} data corresponding to the P_{11} data of Fig. 14; typical power reflections of 60% are obtained over the frequency band of 20 to 21 GHz. This information provides the basis for the design of the transistor output matching network. Typical measurements are plotted in Fig. 15B for transistors fabricated from three different wafers. The spread in the data may be attributed to dissimilarities in these transistors and to measurement uncertainties.

A number of factors contribute to the difficulty in obtaining accurate characterizations of K-Band FETs. The physical size of test-circuits and measurement standards was initially scaled to correspond to transistor dimensions. Fused-silica substrates of .010" thickness were selected to provide 50-ohm microstrip lines whose line width coincided closely with that of the transistor leads utilized by the MSC "small chip-carrier" which was used on initial devices produced in this development program. Consequently, the transistor leads did not contribute significantly to the measurement. However, in order to provide a better input match into the transistor and improve the mechanical characteristics of the partial-packaging configuration, the manufacturer later selected a "large chip-carrier" configuration which utilizes larger standoffs and wider transistor leads. Subsequent characterizations of transistors showed some dependance on transistor lead dimensions since the lead width exceeds the width of the 50-ohm microstrip lines. These effects must be considered to accurately determine FET S-parameters.

An additional factor contributing to measurement uncertainty is that of physical dissimilarites between components used in the calibration of the test system and those associated with test holders. Measurements of calibration standards similar to those used in calibration (but not identical) indicate a typical measurement accuracy of $\pm$ 10% in magnitude and $\pm$ 7° in phase over the 18-22 GHz frequency band for reflection and transmission components with

FREQUENCY (MHz)	MAG P22	ARG P22 (deg)	MAG P21	FORWARD GAIN (dB)	OUTPUT RETURN LOSS (dB)
20000	.79	124.83	.612	-4.27	-2.06
20100	.78	123.24	.667	-3.52	-2.18
20200	.84	128.07	.732	-2.71	-1.52
20300	.87	129.64	.728	-2.76	-1.26
20400	.84	129.79	.724	-2.80	-1.55
20500	.76	131.62	.698	-3.13	-2.39
20600	.76	128.49	.691	-3.21	-2.38
20700	.76	122.83	.737	-2.66	-2.44
20800	.73	120.37	.777	-2.19	-2.78
20900	.76	120.61	.849	-1.42	-2.33
21000	.71	117.09	.885	-1.06	-3.00

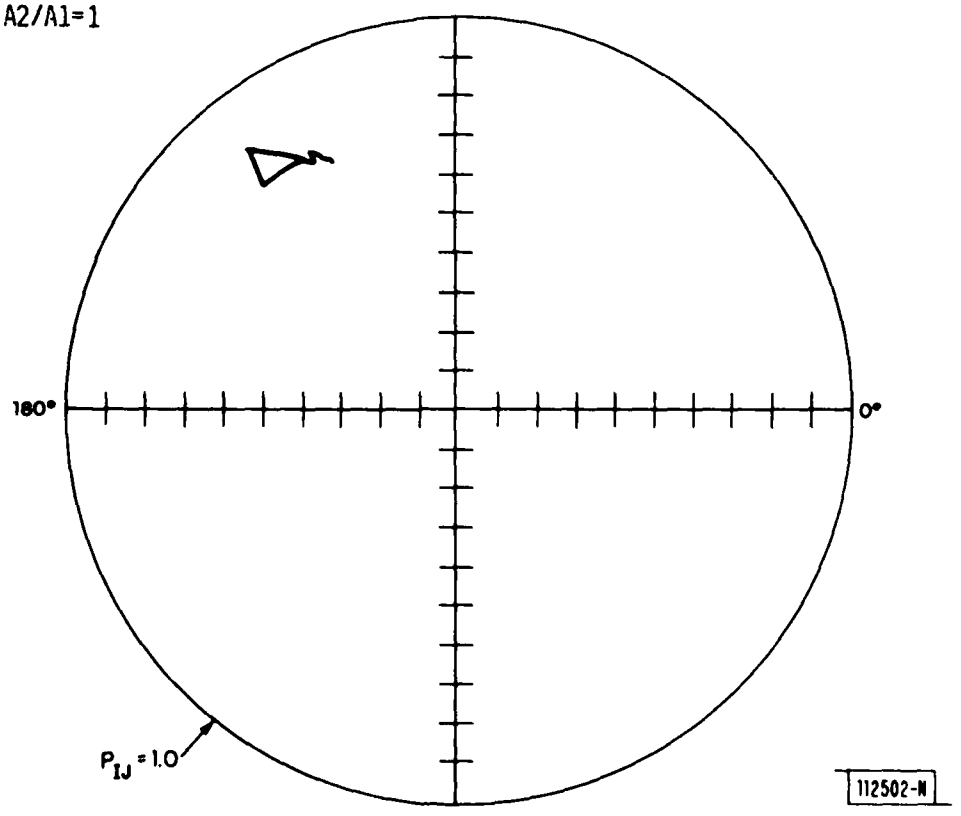

Fig. 15A. P-parameter measurements: K-band 0.5 W FET, P_{22} (50-ohm network installed).

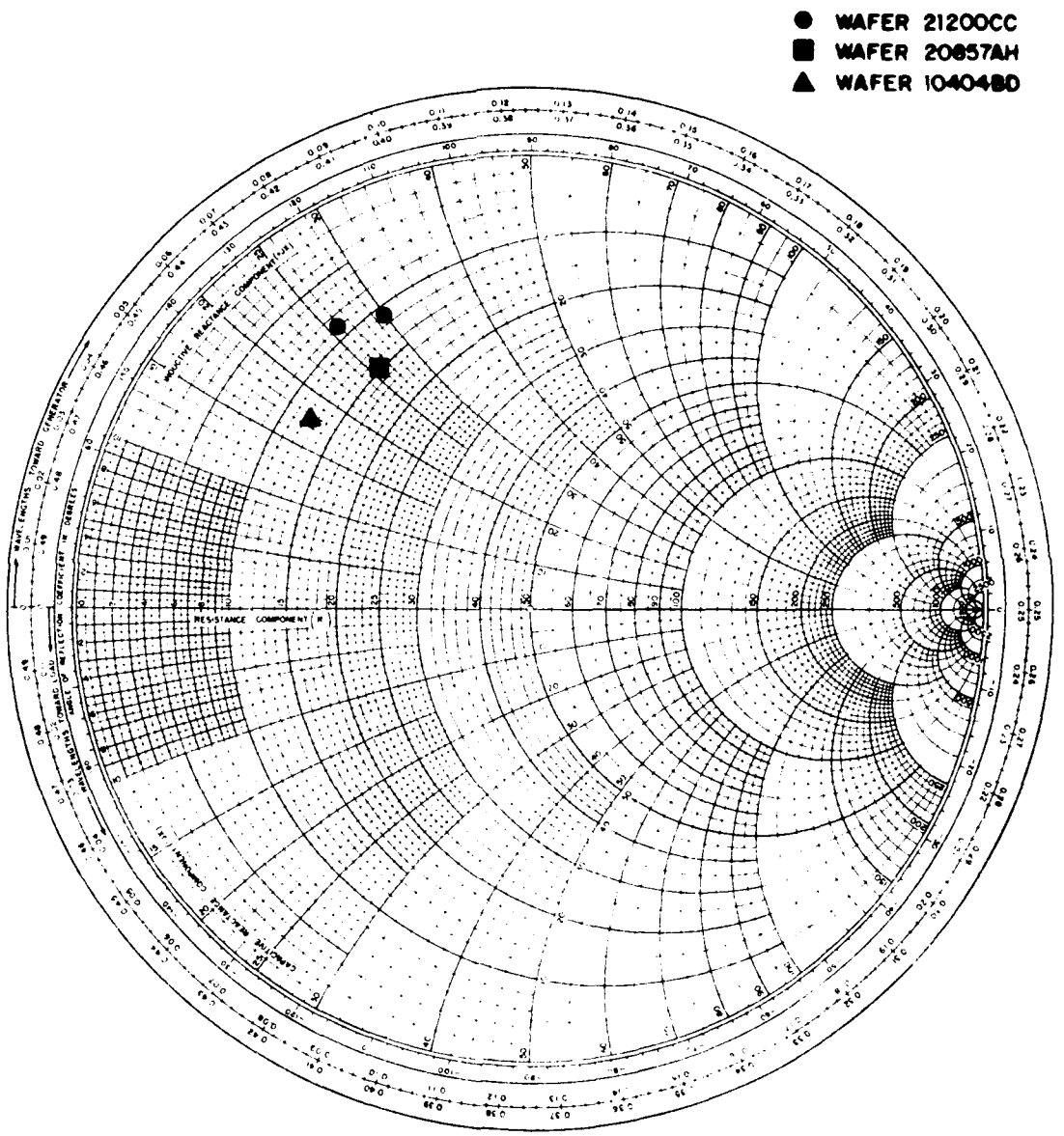

Fig. 15B. P_{22} measurement comparison.

unity coefficients (ignoring line losses) in the microstrip medium. The effects of such an error is shown in Fig. 16 for both a measurement of a standard with unity reflection-coefficient and a typical P_{22} measurement. For such inaccuracies, design iterations spanning the uncertainty in characterizations are required to achieve desired performance.

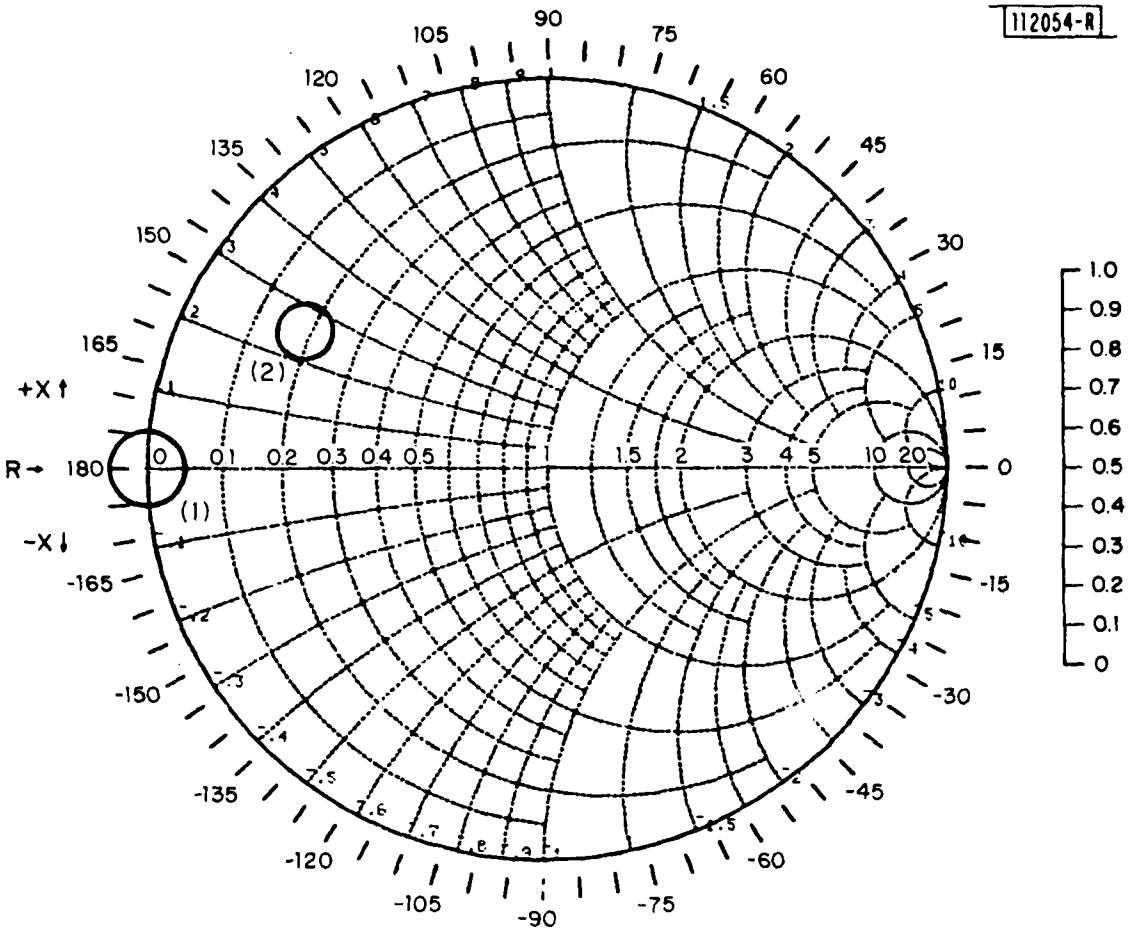

(1) MEASUREMENT UNCERTAINTY FOR "UNITY REFLECTION COEFFICIENT" MICROSTRIP CALIBRATION STANDARD

(2) MEASUREMENT UNCERTAINTY FOR TYPICAL P_{22} MEASUREMENT

Fig. 16. Typical measurement error.

IV. FET PERFORMANCE

On the basis of the large-signal characterizations described previously, matching networks were designed in a microstrip environment to evaluate transistor capability. These designs have been iterated as necessary to accommodate both the uncertainties associated with transistor characterizations and the range of devices under consideration. Transistors selected from four wafers have been tested; some results are listed in Table III for a test frequency of $\approx$ 19 GHz where the best performance was achieved with initial circuit designs. These results include the losses introduced by the matching networks. While there is considerable variance in this data sample, the mean values which are indicated ($\approx$ .5 watt power output, 3.6 dB gain, and 32% power-added efficiency) are representative of transistor performance capability. These test results correspond to matched transistor configurations exhibiting 3 dB bandwidths of typically 300 to 500 MHz. Figure 17 plots typical 19 GHz FET performance which also includes losses of microstrip matching networks. The matching network configuration used in this circuitry is modeled in Fig. 18. These networks are comprised of distributed-element microstrip transmission lines only. Several additional configurations employing fewer matching sections have been investigated with no significant performance advantages realized. The matching networks include a single section of transmission line of appropriate characteristic impedance and length[12] to map the transistor large-signal input or output impedance to a real impedance; this impedance is then matched to 50-ohms using two cascaded quarter-wavelength transformers.

TABLE III

FET PERFORMANCE SUMMARY

WAFER/SN	FREQUENCY	POWER OUTPUT	GAIN	POWER ADDED EFFICIENCY
#	GHz	dBmW	dB	%
20911CE-3	18.87	26.6	3.1	20.5
20911CE-6	18.87	25.8	1.3	10.7
20857AF-4	18.87	26.5	4.5	30.6
20857AH-2	18.87	26.8	3.8	29.2
10404BD-3	18.87	27.9	3.4	30.0
10404BD-5	18.87	26.1	3.6	38.6
10404BD-7	18.87	27.7	3.6	41.4
21200CC-1	18.8	28.6	4.6	40.4
21200CC-9	18.8	24.3	3.7	22.6
21200CC-2	18.87	29.5	4.6	49.7
Mean		27.21	3.62	31.9
Standard Deviation		1.24	0.92	10.7

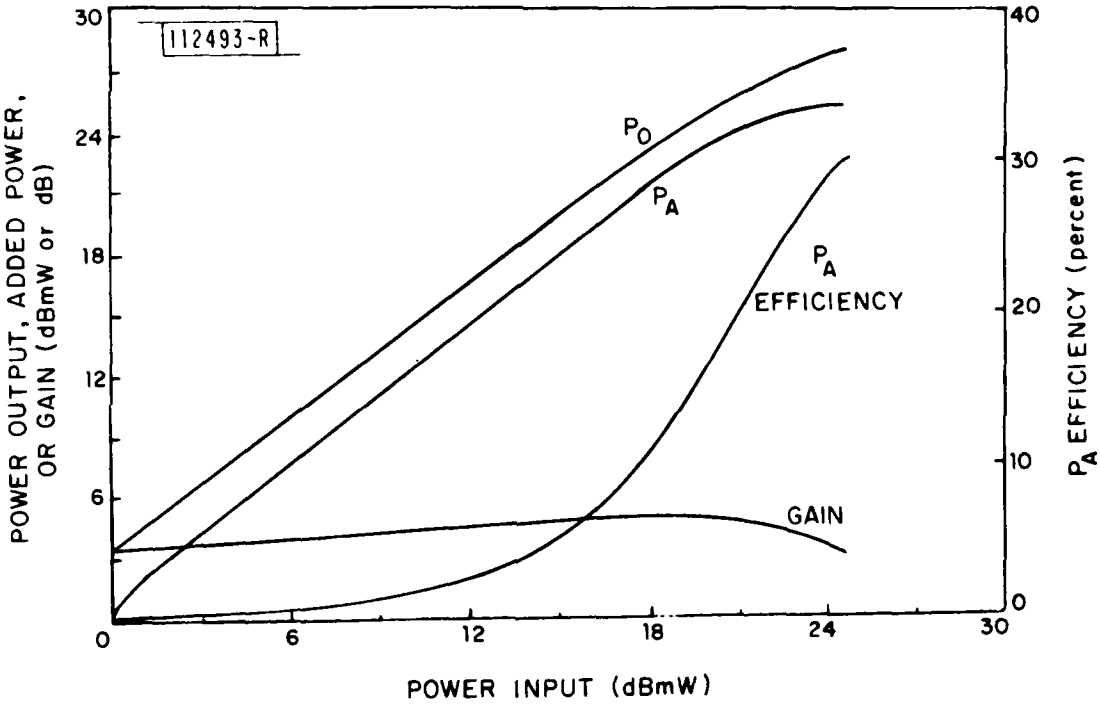

Fig. 17. 19 GHz FET performance.

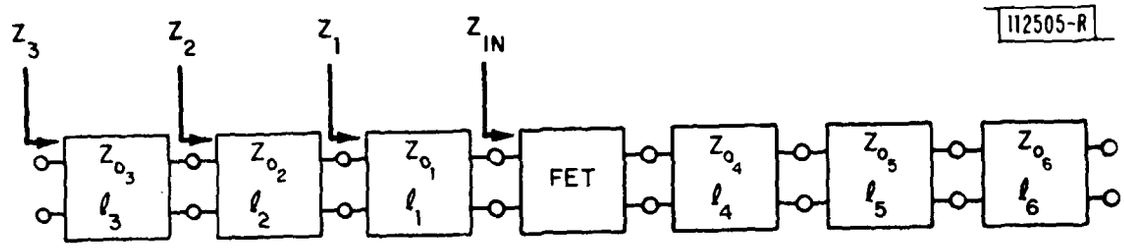

$$Z_{IN} = \frac{(1+S_{11})}{(1-S_{11})} Z_o \qquad Z_2 = \frac{Z_{o_2}^2}{Z_1},$$

$$\ell_2 = \ell_3 = \lambda_{g_o}/4$$

$$Z_{01} = |Z_{IN}|,$$

$$\ell_1 = \lambda_{g_o}/8 \qquad Z_{o_3} = \sqrt{Z_G Z_2}$$

$$Z_1 = \frac{RE\{Z_{in}\}}{1 - \frac{IM\{Z_{in}\}}{|Z_{in}|}}$$

Fig. 18. Circuit model for FET impedance matching networks and design approximations.

V. AMPLIFIER DESIGN AND PERFORMANCE

A complete experimental amplifier stage requires a means of biasing both the gate and the drain of the field-effect transistor. Bias blocking and insertion networks were designed which utilize coupled microstrip lines in conjunction with a T-junction high-impedance feedline interconnected to a commercially-available feedthru filter by a conductor loaded with a single ferrite bead (Fig. 19A). The performance of these bias networks is shown in Fig. 19B; typical loss of ≈ 1.0 dB was achieved in the frequency band of 20-21 GHz. This performance includes the loss of two coaxial to microstrip launchers which contribute most of the loss. A circuit model for the bias network is shown in Fig. 20.

To complete the experimental amplifier design, the bias networks were fabricated on the same fused-silica substrates (.5" x .5" x .010") with the input or output matching networks for the transistor (see Fig. 21). Impedance-compensation networks were included as necessary to accommodate the interface of matching networks, bias networks, and coaxial to microstrip launchers. All of these networks utilize distributed element microstrip transmission lines only.

The performance of several complete experimental amplifier stages is summarized in Table IV. Devices from wafer #21200 CC consistently performed better than devices from the other three wafers which were evaluated in this circuit design. For the best wafer, average performance of 0.4 watt power output at 3.0 dB gain and ≈ 15% power-added efficiency was achieved at 20 GHz. Best performance results include 0.5 watt power output at 16.4% power-added efficiency. Typical amplifier performance is plotted in Fig. 22 as a function of power input. Maximum power-added efficiency for this amplifier occurs at ≈ 2 dB compression from typical linear gain of 5.0 dB.

The power-bandwidth responses of Fig. 23 show the 1 dB bandwidth of this amplifier to be in excess of 1 GHz at typical operating input power levels (+22 to +24 dBmW) with midband gain of ≈ 3.0 dB. Some bandwidth shrinkage is noted for large decreases in power input (> 10 dB reduction).

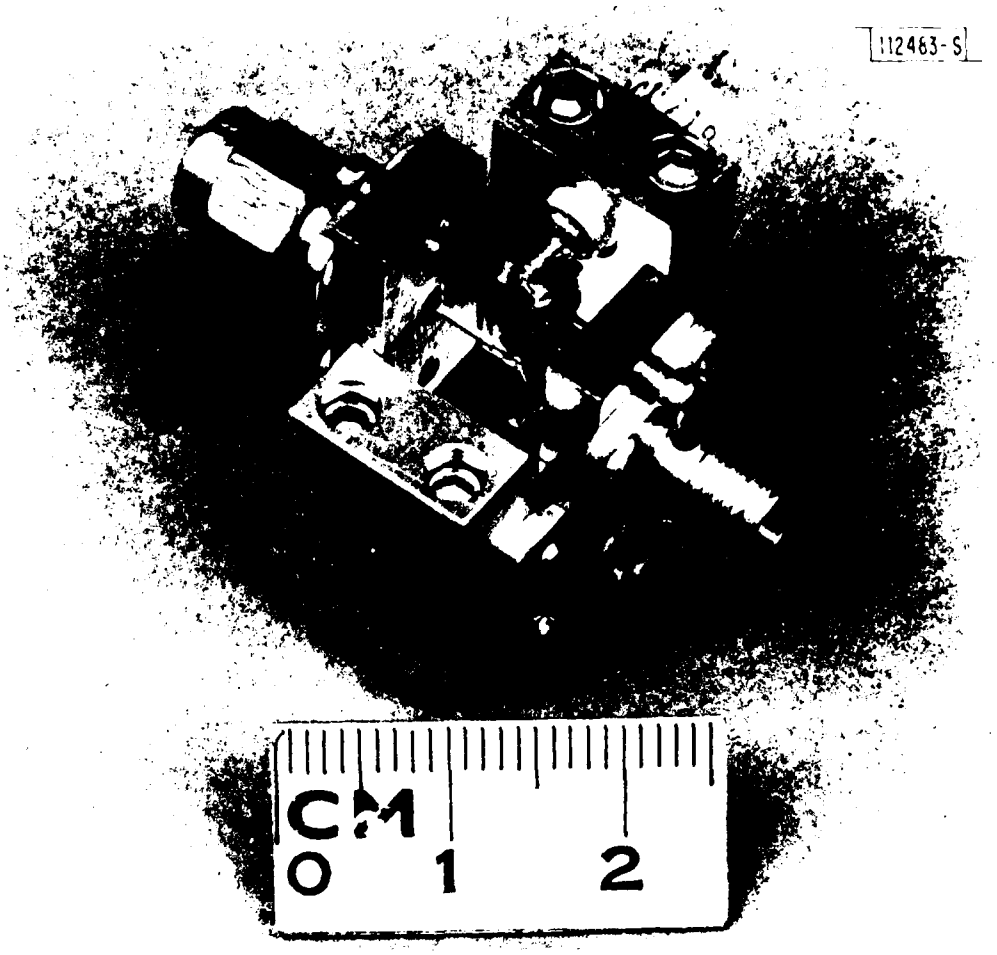

Fig. 19A. Microstrip bias network.

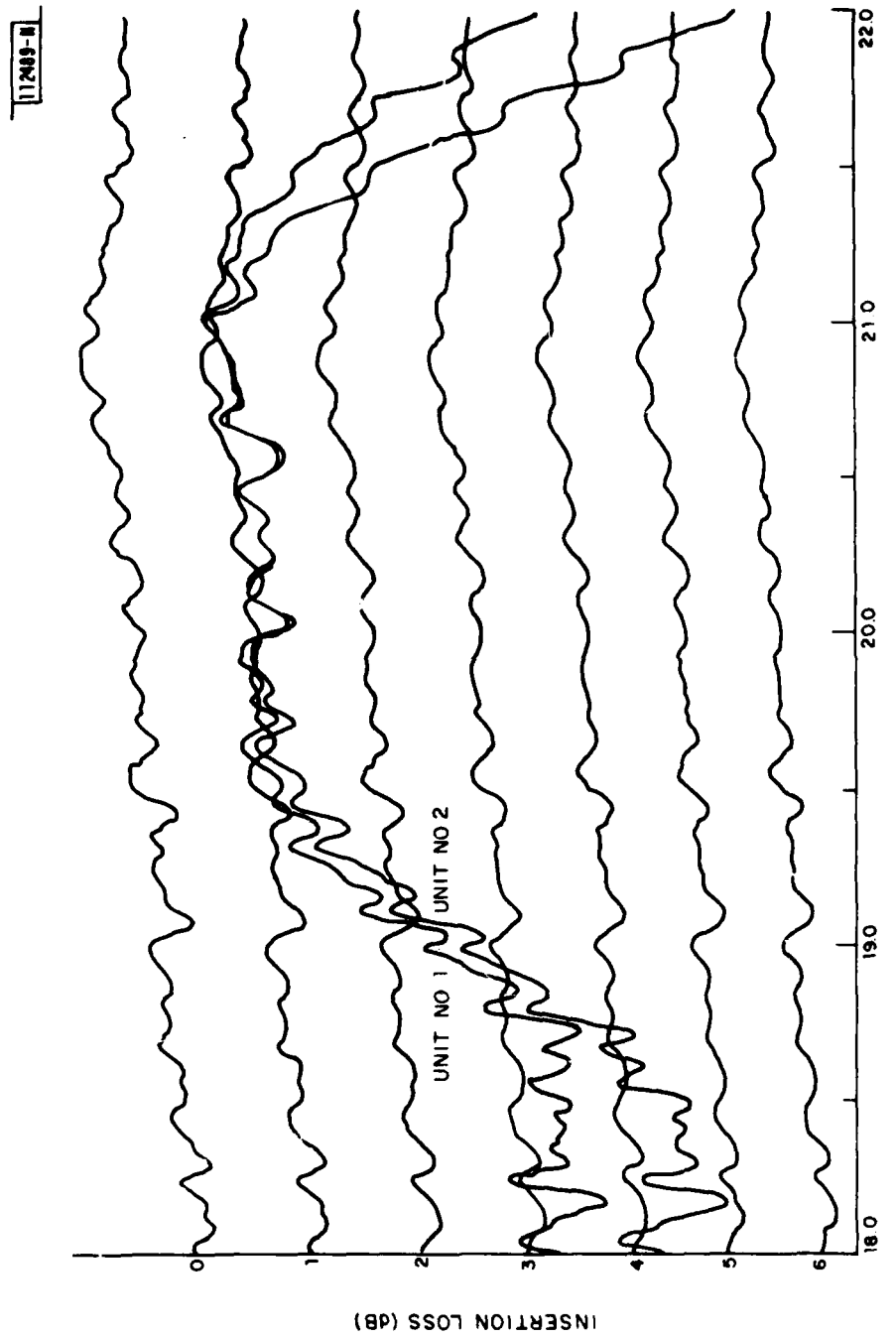

Fig. 19B. Performance of microstrip bias networks.

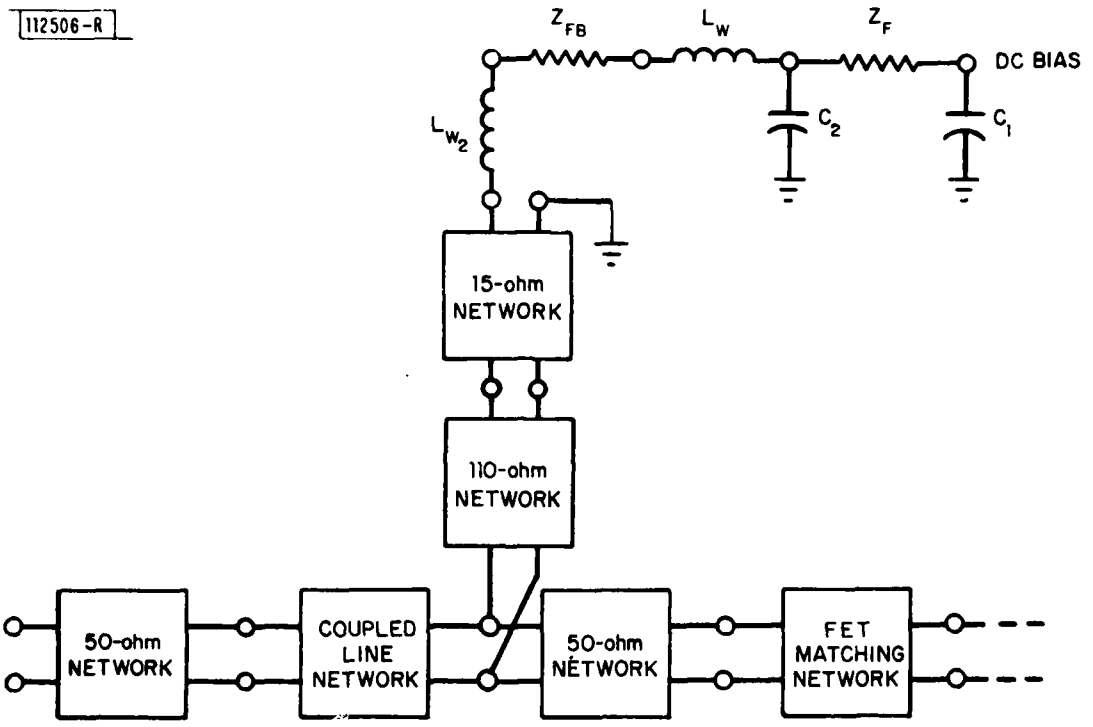

Fig. 20. Circuit model for bias network.

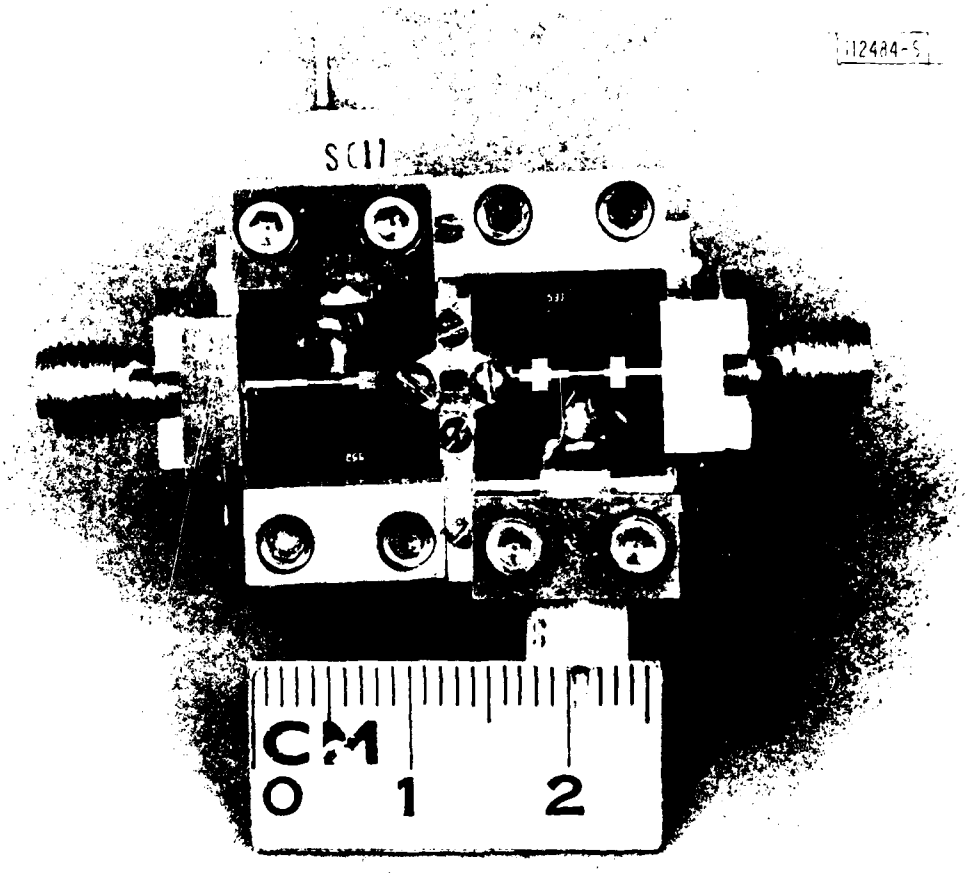

Fig. 21. Experimental microstrip amplifier.

TABLE IV

MICROSTRIP AMPLIFIER PERFORMANCE SUMMARY

Wafer/SN #	Circuit #	Frequency (GHz)	Power Output (dBmW)	Gain (dB)	Power-Added Efficiency (%)	1 dB Bandwidth (GHz)
21200CC-1	225/231	20.2	26.5	3.0	14.0	1.2
21200CC-2	225/231	19.7	26.1	3.0	18.1	1.4
21200CC-7	225/231	20.0	27.0	3.0	16.4	1.5
21200CC-8	225/231	20.1	25.0	3.0	13.1	0.8
21200C-F10	225/231	20.2	25.3	2.8	14.4	0.9
21200C-F13	225/231	20.1	23.9	1.9	9.6	0.8
10404BD-3	225/231	20.9	24.0	2.0	7.4	0.9
10404BD-7	233/236	21.1	24.1	2.1	10.0	0.8
20857AH-2W	225/231	20.2	25.0	2.0	9.0	1.4
20857AH-23W	225/242	20.7	24.2	2.2	8.4	1.0

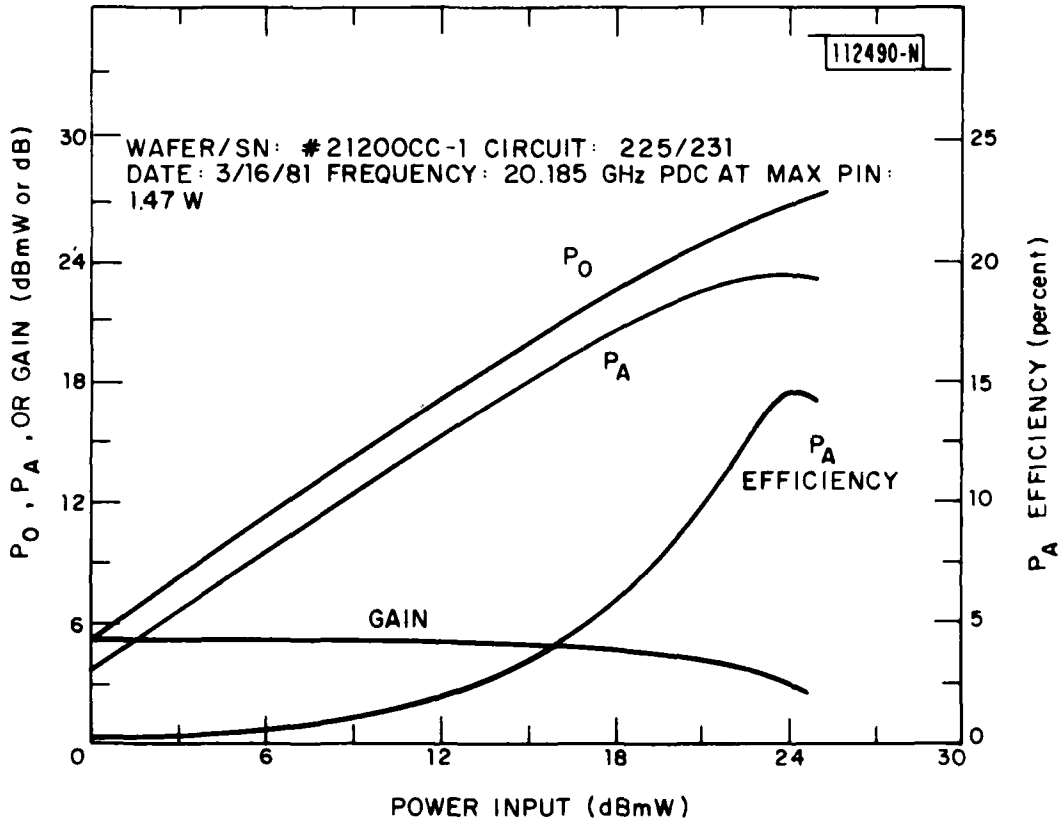

Fig. 22. Microstrip amplifier performance.

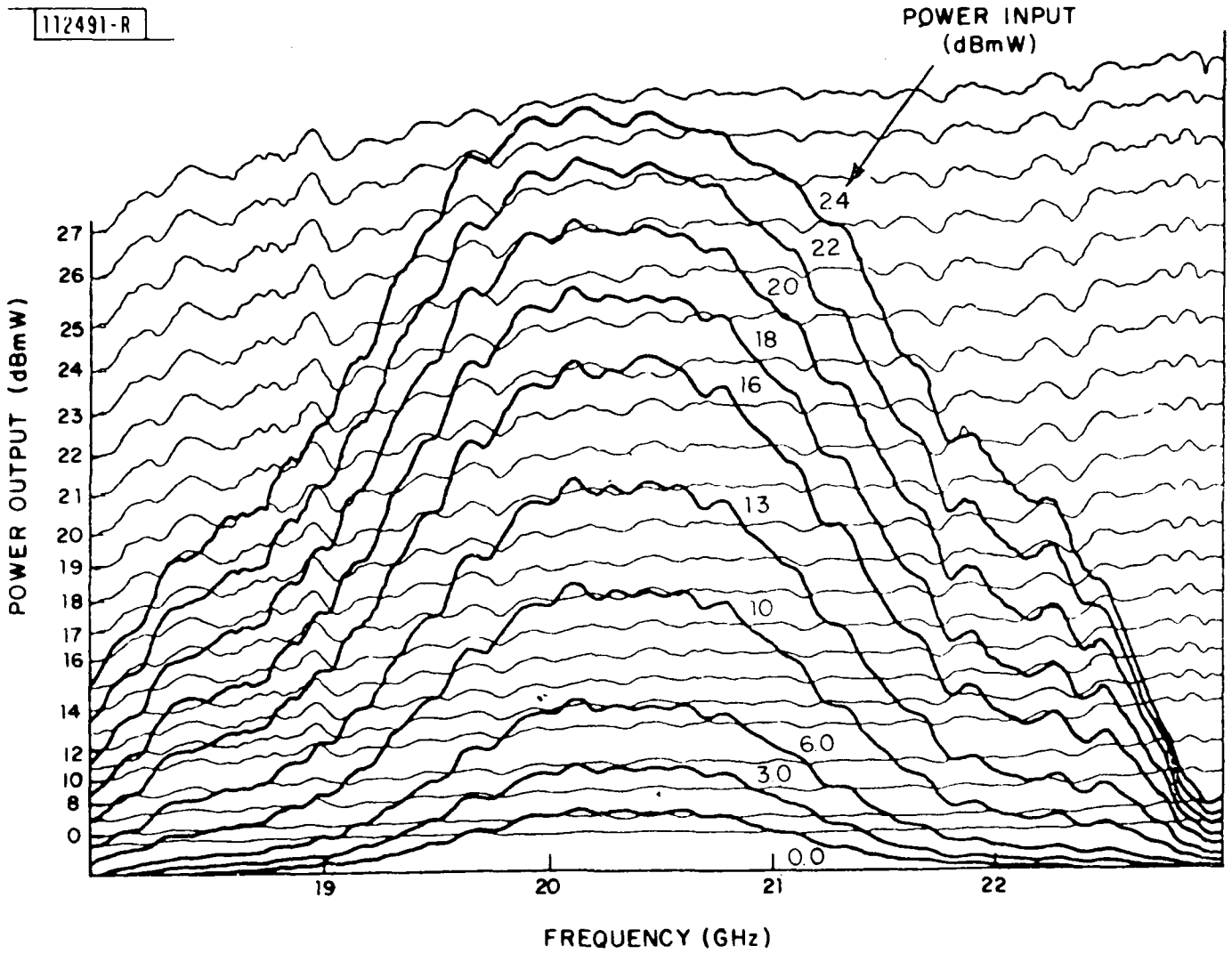

Fig. 23. Microstrip amplifier power-bandwidth response.

The large-signal S-parameter measurements for the complete amplifier are listed in Table V together with calculated performance parameters. These measurements were made using 3.5 mm coaxial standards and correspond to performance referenced to the input and output of the coaxial connections to the amplifier. The input return-loss is plotted in Fig. 24A; it exceeds 10 dB in the 1 GHz band centered at ≈ 20.4 GHz, while the gain calculated from these measurements approaches 4 dB at a power input of +21 dBmW (Fig. 24B). The amplifier bandwidth appears to be limited by the input match. The average group-delay for the complete amplifier stage also calculated from the large-signal S-parameter measurements ($\not\exists S_{21}$) for a 1 GHz band centered at 20.5 GHz was determined to be ≈ .5 nanosecond.

Temperature cycling of the amplifier stage yielded the power output variations shown in Fig. 25 measured over the frequency band from 19.8 to 21.8 GHz. Typical variations of 1 dB are observed in the power output at the center of the operating band over the temperature range of -40°C to +60°C. This variation increased to ≈ 2 dB at the band edges of the 1 GHz operating band.

Additional packaging requirements were necessary beyond those employed in the experimental amplifier configuration to completely enclose the amplifier stage. Evaluation of initial package design indicated the presence of waveguide mode propagation and necessitated the reduction in substrate width shown in Fig. 26 to establish a waveguide beyond cutoff when the cover is installed. After making the reduction in substrate width, a completely-enclosed amplifier stage yielded the expected performance and no anomalies were observed.

TABLE VA

LARGE-SIGNAL S-PARAMETERS AND CALCULATED PERFORMANCE FOR MICROSTRIP AMPLIFIER

	S11		S21		S12		S22	
frequency	mag	angle	mag	angle	mag	angle	mag	angle
18000	.54	61	.27	115	.00	70	2.66	-137
18100	.44	46	.20	106	.01	121	.91	-65
18200	.53	33	.26	101	.01	105	.90	-73
18300	.51	19	.29	89	.01	92	.89	-81
18400	.54	6	.35	76	.01	82	.91	-90
18500	.54	-7	.40	58	.02	68	.88	-100
18600	.55	-24	.43	43	.01	56	.88	-109
18700	.50	-42	.46	30	.02	46	.87	-120
18800	.49	-63	.54	17	.01	34	.86	-130
18900	.48	-80	.59	1	.02	31	.86	-141
19000	.48	-88	.66	-16	.02	3	.84	-154
19100	.47	-105	.77	-28	.02	-11	.82	-165
19200	.46	-123	.90	-41	.02	-21	.79	-178
19300	.49	-136	.93	-53	.03	-33	.78	170
19400	.49	-150	.96	-71	.03	-42	.75	156
19500	.46	-164	1.03	-91	.03	-64	.68	140
19600	.39	179	1.16	-105	.04	-74	.62	121
19700	.41	162	1.31	-128	.05	-91	.67	98
19800	.36	142	1.34	-153	.06	-110	.51	68
19900	.25	126	1.38	-174	.06	-130	.41	34
20000	.20	109	1.56	170	.07	-152	.38	12
20100	.16	102	1.63	151	.07	-172	.37	-12
20200	.10	97	1.57	127	.08	172	.39	-58
20300	.06	32	1.61	102	.08	149	.45	-94
20400	.08	-66	1.43	80	.07	128	.45	-125
20500	.12	-72	1.46	64	.07	110	.51	-145
20600	.13	-80	1.34	49	.07	91	.57	-165
20700	.19	-99	1.40	29	.06	71	.57	174
20800	.27	-125	1.36	11	.05	56	.60	155
20900	.31	-138	1.26	-2	.05	40	.64	140
21000	.37	-155	1.13	-16	.05	20	.66	126
21100	.41	-164	1.07	-30	.04	5	.64	113
21200	.50	-171	1.07	-51	.04	-9	.66	100
21300	.55	-178	1.05	-74	.04	-28	.65	86
21400	.58	172	.91	-89	.03	-47	.67	72
21500	.61	161	.85	-99	.03	-63	.68	58
21600	.61	151	.82	-117	.03	-76	.63	45
21700	.60	141	.91	-134	.03	-89	.62	32
21800	.62	131	.91	-156	.03	-107	.61	19
21900	.62	125	.87	-175	.03	-130	.55	13
22000	.62	117	.87	168	.03	-154	.49	8

TABLE VB

LARGE-SIGNAL S-PARAMETERS AND CALCULATED PERFORMANCE FOR MICROSTRIP AMPLIFIER

225/231 #2120CC-1

DATE=

REF PLANE= 0.0 RF P(IN)= 21.0

VG= -1.07 VD= 8.54 ID= .244

FREQUENCY	RETLO IN	PHASE	GAIN	PHASE	REV GAIN	PHASE	RETLO OUT	PHASE
18003	5.43	61	-11.38	115	-48.86	70	-8.49	-137
18103	7.06	49	-13.94	106	-44.86	121	.78	-65
18203	5.49	33	-11.68	101	-39.70	105	.89	-73
18303	5.79	19	-10.85	89	-39.66	92	.98	-81
18403	5.40	6	-9.20	76	-39.04	82	.86	-90
18503	5.32	-7	-7.99	58	-36.47	68	1.14	-100
18603	5.26	-24	-7.35	43	-36.72	56	1.10	-109
18703	6.04	-42	-6.80	30	-36.15	46	1.24	-120
18803	6.23	-63	-5.41	17	-36.48	34	1.28	-130
18903	6.31	-80	-4.53	1	-35.37	31	1.30	-141
19003	6.38	-88	-3.61	-16	-34.28	3	1.52	-154
19103	6.52	-105	-2.24	-28	-33.90	-11	1.68	-165
19203	6.75	-123	-.94	-41	-32.77	-21	2.03	-178
19303	6.11	-136	-.61	-53	-30.49	-33	2.19	170
19403	6.17	-150	-.39	-71	-29.97	-42	2.50	156
19503	6.83	-164	.23	-91	-29.55	-64	3.40	140
19603	8.08	179	1.32	-105	-29.03	-74	4.17	121
19703	7.72	162	2.33	-128	-26.33	-91	4.86	98
19803	8.90	142	2.53	-153	-24.49	-110	5.82	68
19903	11.99	126	2.77	-174	-24.10	-130	7.65	34
20003	13.83	109	3.85	170	-23.50	-152	8.52	12
20103	16.08	102	4.22	151	-22.86	-172	8.61	-12
20203	19.72	97	3.89	127	-22.15	172	8.15	-58
20303	25.09	32	4.11	102	-21.47	149	6.98	-94
20403	22.18	-66	3.13	80	-22.72	128	6.85	-125
20503	18.14	-72	3.27	64	-23.25	110	5.81	-145
20603	18.01	-80	2.55	49	-23.00	91	4.84	-165
20703	14.35	-99	2.94	29	-24.96	71	4.90	174
20803	11.41	-125	2.68	11	-25.77	56	4.48	155
20903	10.21	-138	2.00	-2	-25.70	40	3.84	140
21003	8.54	-155	1.10	-16	-26.50	20	3.55	126
21103	7.69	-164	.59	-30	-28.01	5	3.89	113
21203	6.01	-171	.55	-51	-28.45	-9	3.61	100
21303	5.12	-178	.40	-74	-28.70	-28	3.74	86
21403	4.73	172	-.81	-89	-29.79	-47	3.45	72
21503	4.30	161	-1.46	-99	-29.84	-63	3.40	58
21603	4.22	151	-1.71	-117	-31.32	-75	3.98	45
21703	4.49	141	-.79	-134	-32.04	-89	4.09	32
21803	4.17	131	-.84	-156	-30.71	-107	4.28	19
21903	4.13	125	-1.18	-175	-30.37	-130	5.15	13
22003	4.09	117	-1.24	168	-30.41	-154	6.27	8

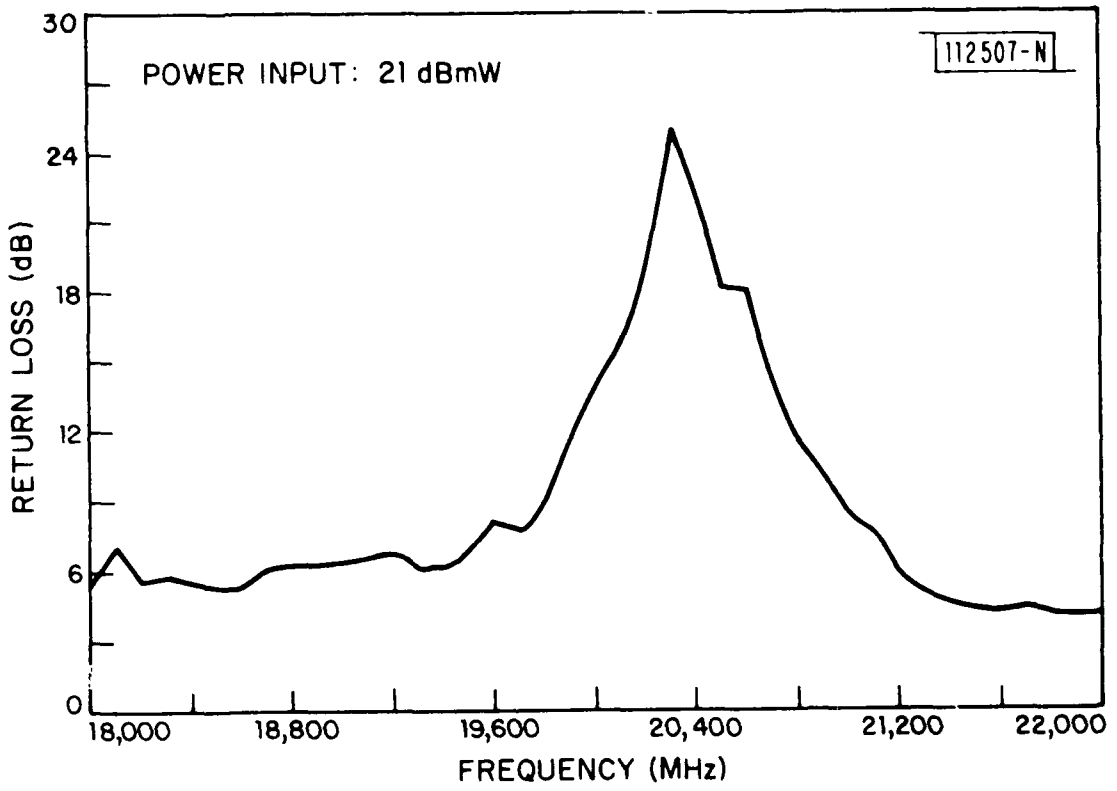

Fig. 24A. Input return-loss for microstrip amplifier.

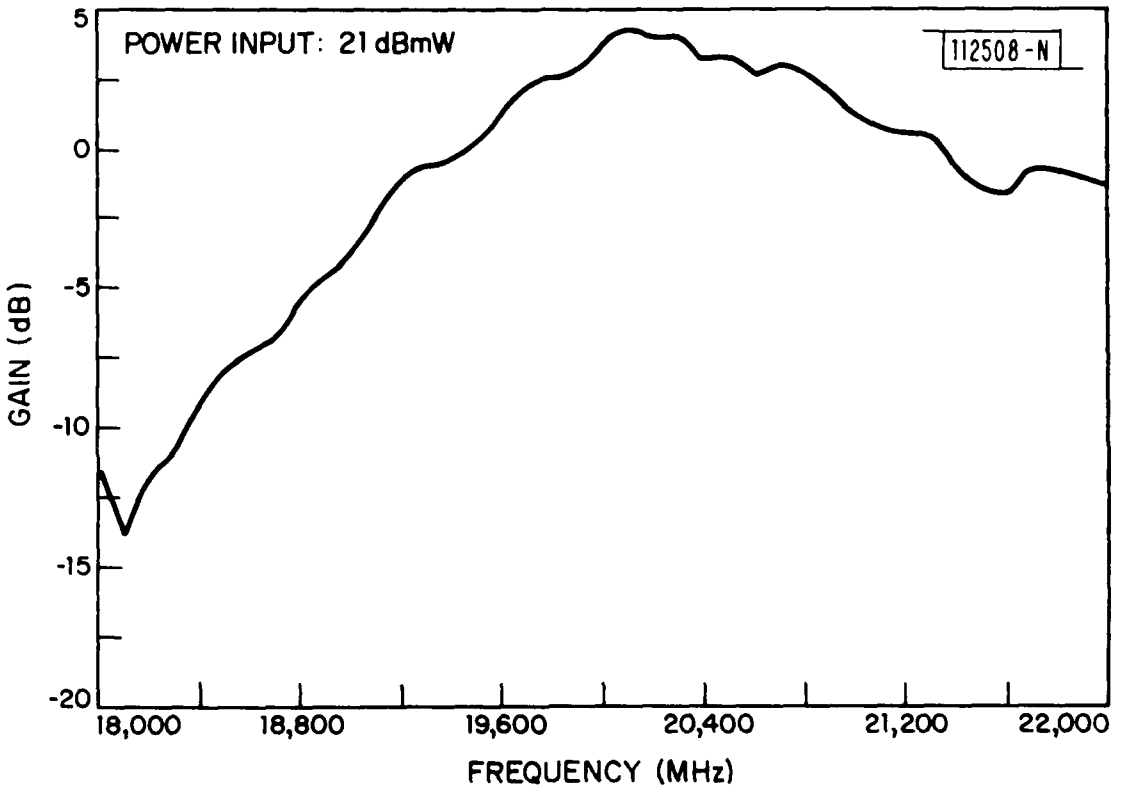

Fig. 24B. Gain of microstrip amplifier calculated from large-signal s-parameter measurements.

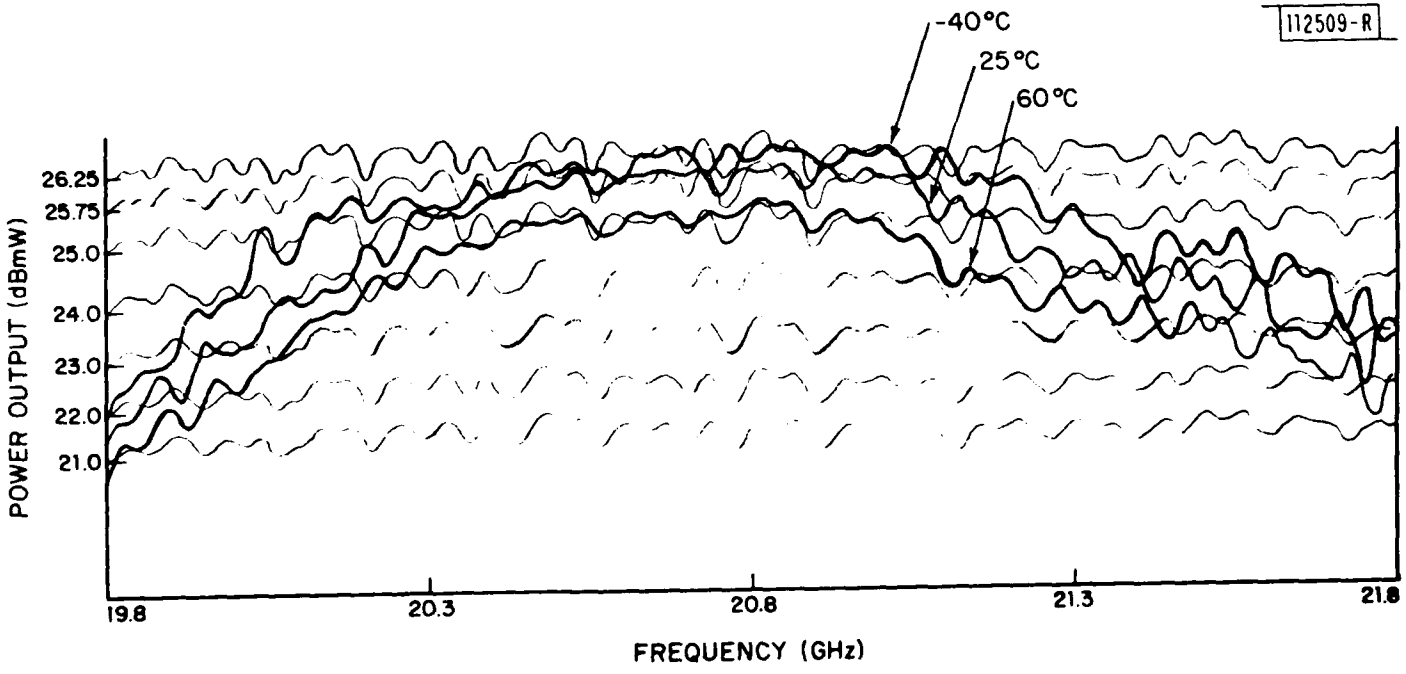

Fig. 25. Temperature effects on microstrip amplifier performance.

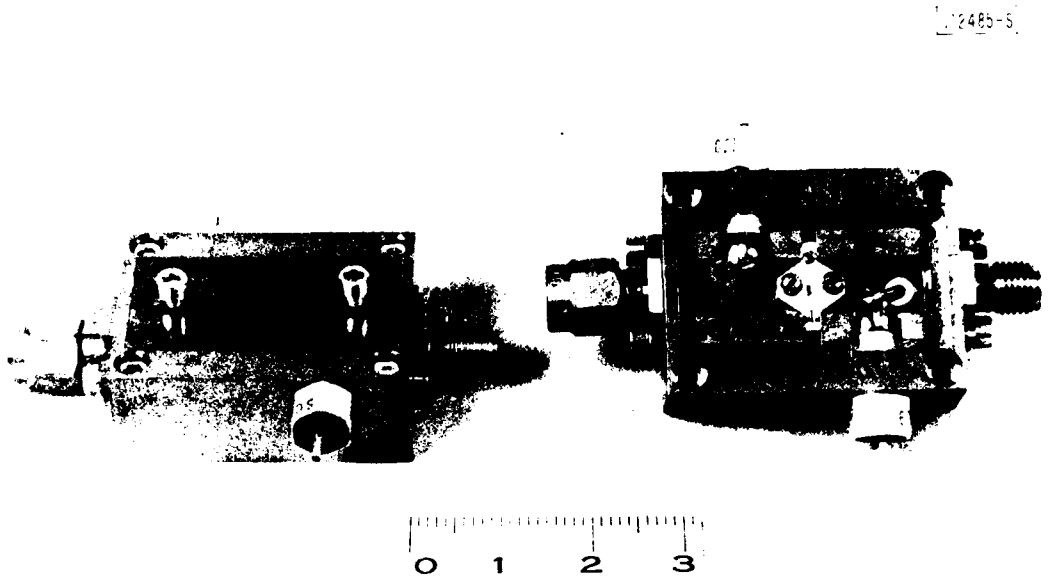

Fig. 26. Packaged microstrip amplifier.

VI. CONTINUING DEVELOPMENT

A primary goal of this development effort is to produce a multi-stage amplifier module meeting specifications for use in a multi-element phased-array satellite downlink transmitter configuration[13]. In pursuit of that goal, additional FET development contracts were granted in October 1980. Microwave Semiconductor Corporation received both a contract for 1.0 watt FET development and for high-gain medium-power (10 dB, 100 mW) transistors. Hughes Aircraft Company and Dexcel, Incorporated also received contracts for the latter. All contracts are presently scheduled for completion by October 1981, (see Appendix A).

At present, the primary emphasis in circuit development centers on cascading amplifier stages. Preliminary tests for two cascaded discrete amplifier stages have yielded 0.4 watt power output at 7 dB gain, and 10 dB small signal gain (Fig. 27). Integration of amplifier stages into a compact package is in progress. The circuit configuration of Fig. 28 easily permits cascading of stages as the amplifier chain is assembled. Each section includes a half-inch fused-silica substrate with appropriate biasing and impedance-matching networks. The proposed multi-stage amplifier configuration will utilize transistors from the development contracts scheduled for completion in October 1981, in addition to the 0.5 watt transistors already developed. The four cascaded amplifier stages shown in Fig. 29 are expected to produce .4 to .6 W of power output with $\approx$ 22 dB of overall gain. The overall power-added efficiency goal for this amplifier module is 15%. Four of these modules will be used in conjunction with the phase shifters shown in the block diagram as part of a phased-array demonstration.

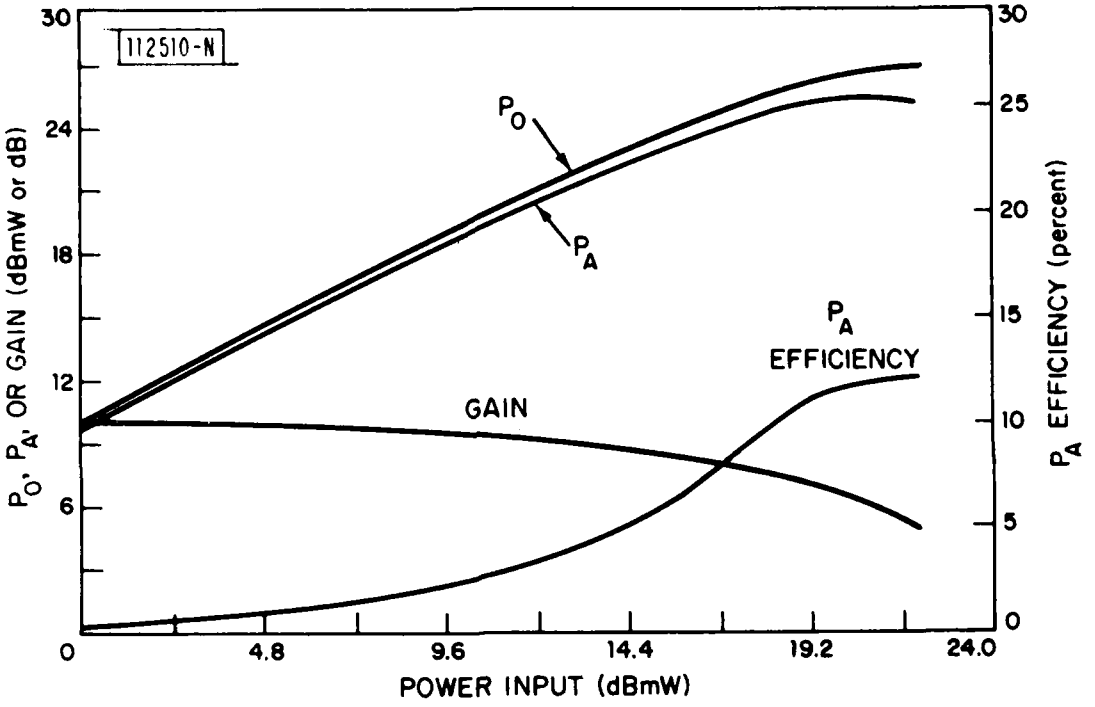

Fig. 27. Performance of two discrete cascaded microstrip amplifier stages.

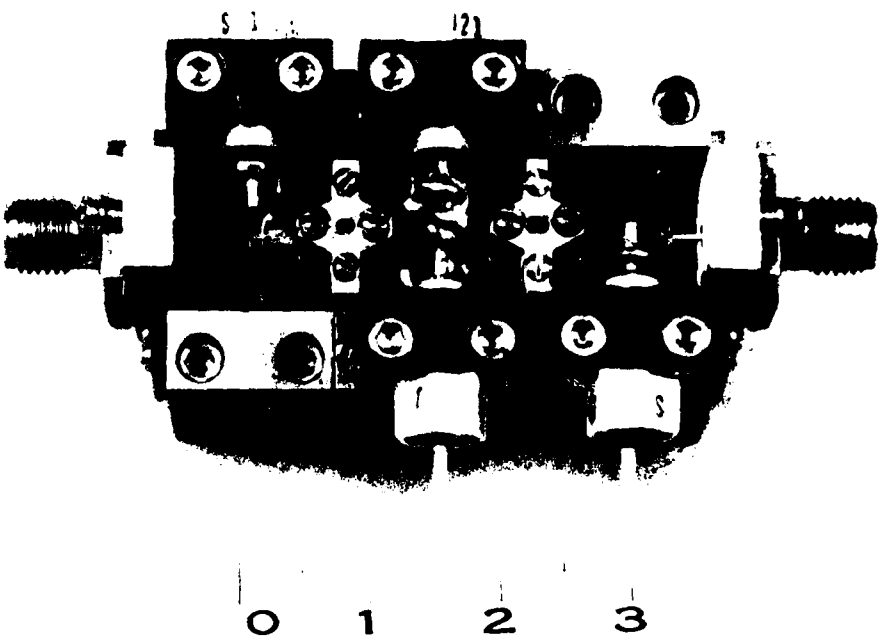

Fig. 28. Experimental two-stage microstrip amplifier.

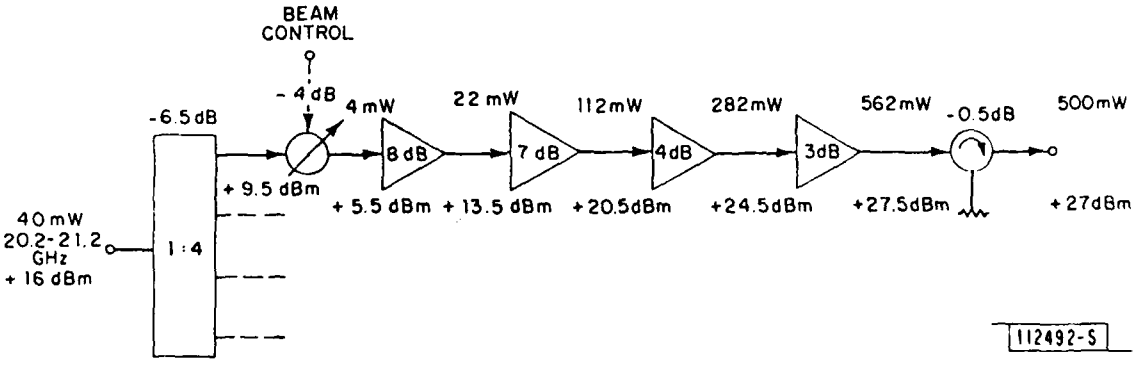

Fig. 29. 20 GHz transmitter test-bed.

VII. CONCLUSION

A K-Band GaAs MESFET development program has produced devices with a typical performance capability of 0.5 watt power output at 3.6 dB gain and 32% power-added efficiency at ≈ 19.0 GHz. A technique for acquiring large-signal characterizations of these devices has been developed. Microstrip amplifier designs have been realized which produce typical performance of 0.4 watt power output at 3.0 dB gain and 15% power added efficiency at 20 GHz. Additional lower-power high-gain FETs are presently under development for the first two stages of multi-stage amplifier modules to be used in a multi-element phased-array satellite transmitter configuration.

APPENDIX A

SUMMARY OF PERFORMANCE SPECIFICATIONS FOR K-BAND DEVELOPMENT PROGRAMS

	I		II		III	
PERFORMANCE AT 21 GHz	GOAL	MINIMUM	GOAL	MINIMUM	GOAL	MINIMUM
Power Output	1.0 W.	0.5 W.	--	1.0 W.	--	0.1 W.
Power Added Efficiency	20%	15%	20%	15%	20%	--
Gain	5.0 dB	4.0 dB	5.0 dB	4.0 dB	10 dB	8 dB
Channel Temperature Rise	< 100°C		< 100°C		< 100°C	
Deliverables	50		60		100	
Contractor	MSC		MSC		MSC Dexcel Hughes	
Status	Completed August 1980		Scheduled Completion October 1981			

APPENDIX B

PERFORMANCE PARAMETERS CALCULATED FROM
SMALL SIGNAL S-PARAMETER MEASUREMENTS

ROLLET'S STABILITY FACTOR (K)

$$K = \frac{1 + |S_{11}\,S_{22} - S_{12}\,S_{21}|^2 - |S_{11}|^2 - |S_{22}|^2}{2\,|S_{12}|\,|S_{21}|} \tag{17}$$

$K < 1$, Potentially Unstable

$K > 1$, Unconditionally Stable

MAXIMUM AVAILABLE GAIN (MAG)

$$MAG = \left|\frac{S_{21}}{S_{12}}\right| (K - \sqrt{K^2 - 1} \tag{18}$$

MAXIMUM STABLE GAIN (MSG)

$$MSC = \left|\frac{S_{21}}{S_{12}}\right| \tag{19}$$

$$K > 1,\ K = \frac{1}{2}\left(\frac{MSG}{MAG} + \frac{MAG}{MSG}\right)$$

ACKNOWLEDGEMENTS

The author is grateful for the assistance of several people who have contributed to this work. Error-correction of measurement data by desktop computer results largely from the contributions of Dr. Peter W. Staecker. Dr. Ronald F. Bauer furnished a suitable algorithm for the data reduction of two signal measurements. David M. Hodsdon provided assistance in the analysis of multiple coupled microstrip lines. Dr. Ira Drukier and Dr. Leonard Rosenheck of Microwave Semiconductor Corporation are responsible for the design and fabrication of the GaAs FETs and also provided many helpful discussions. Timothy J. King made many of the measurements and provided circuit fabrication assistance together with William Macropoulos, William L. McGilvary, and William E. Fielding. Michael Demerjian provided assistance with data processing requirements.

REFERENCES

1. S. R. Mazumder and P. D. Van der Puije, ""Two-Signal" Method of Measuring the Large-Signal S-parameters of Transistors," IEEE Trans Microwave Theory Tech. MTT-26, 417 (1978).

2. Technical Proposal: "K-Band FET Development," prepared by Microwave Semiconductor Corporation for M.I.T. Lincoln Laboratory, (May 1979).

3. Ibid.

4. "K-Band FET Development Final Report," prepared by Microwave Semiconductor Corporation for M.I.T. Lincoln Laboratory, (August 1980).

5. M. L. Stevens, "Characterization of Power MESFETs at 21 GHz," TR-579, Lincoln Laboratory M.I.T. Technical Report (15 September 1981).

6. Stig Rehnmark, "On the Calibration Process of Automatic Network Analyzer Systems," IEEE Trans. Microwave Theory Tech. MTT-22, 457 (1974).

7. R. F. Bauer and P. Penfield, Jr., "De-Embedding and Unterminating," IEEE Trans. Microwave Theory Tech. MTT-22, 282 (1974).

8. "S-parameters ... Circuit Analysis and Design," HP Application Note 95, September 1968.

9. See Reference 1.

10. K. Kurokawa, "Power Waves and the Scattering Matrix," IEEE Trans. Microwave Theory Tech. MTT-13, 194 (1965).

11. Notation suggested by D. Peck of Watkins-Johnson at IEEE Symposium Power GaAs FET Workshop, Los Angeles, CA, June 19, 1981.

12. D. H. Steinbrecher, "An Interesting Impedance Matching Network," IEEE Trans. Microwave Theory Tech. MTT-15, 382 (1967).

13. P. R. Hirschler-Marchand, C. D. Berglund, M. L. Stevens, "System Design and Technology Development for An EHF Beam-Hopped Satellite Downlink," National Telecommunications Conference Record, Vol. 1, Sect. 17.5, Houston TX, November 1980.

UNCLASSIFIED

SECURITY CLASSIFICATION OF THIS PAGE *(When Data Entered)*

REPORT DOCUMENTATION PAGE		READ INSTRUCTIONS BEFORE COMPLETING FORM
1. REPORT NUMBER ESD-TR-81-296	2. GOVT ACCESSION NO. AD-A110	3. RECIPIENT'S CATALOG NUMBER 873
4. TITLE *(and Subtitle)* Large-Signal Characterization, Amplifier Design, and Performance of K-Band GaAs MESFETS		5. TYPE OF REPORT & PERIOD COVERED Technical Report 6. PERFORMING ORG. REPORT NUMBER Technical Report 586
7. AUTHOR(S) Carl D. Berglund		8. CONTRACT OR GRANT NUMBER(S) F19628-80-C-0002
9. PERFORMING ORGANIZATION NAME AND ADDRESS Lincoln Laboratory, M.I.T. P.O. Box 73 Lexington, MA 02173		10. PROGRAM ELEMENT, PROJECT, TASK AREA & WORK UNIT NUMBERS Program Element Nos. 33601F and 63431F Project Nos. 2487 and 2028
11. CONTROLLING OFFICE NAME AND ADDRESS Air Force Systems Command, USAF Andrews AFB Washington, DC 20331		12. REPORT DATE 11 December 1981 13. NUMBER OF PAGES 70
14. MONITORING AGENCY NAME & ADDRESS *(if different from Controlling Office)* Electronic Systems Division Hanscom AFB Bedford, MA 01731		15. SECURITY CLASS. *(of this report)* Unclassified 15a. DECLASSIFICATION DOWNGRADING SCHEDULE

16. DISTRIBUTION STATEMENT *(of this Report)*

Approved for public release; distribution unlimited.

17. DISTRIBUTION STATEMENT *(of the abstract entered in Block 20, if different from Report)*

18. SUPPLEMENTARY NOTES

None

19. KEY WORDS *(Continue on reverse side if necessary and identify by block number)*

FET	GaAs	microstrip
MESFET	Large-signal S-parameters	power amplifier
K-Band		

20. ABSTRACT *(Continue on reverse side if necessary and identify by block number)*

Recent advances in Gallium Arsenide field-effect transistor technology have extended the power amplification capabilities of FETs to the K-Band frequency range. FETs with performance capability of 1 watt power output at 20 GHz have been developed. Large-signal S-parameter characterizations of these devices have been utilized in designing power amplifiers. Transistor performance capability is discussed together with the performance of experimental amplifier designs realized in a microstrip configuration.

DD FORM 1473 EDITION OF 1 NOV 65 IS OBSOLETE

UNCLASSIFIED

SECURITY CLASSIFICATION OF THIS PAGE *(When Data Entered)*

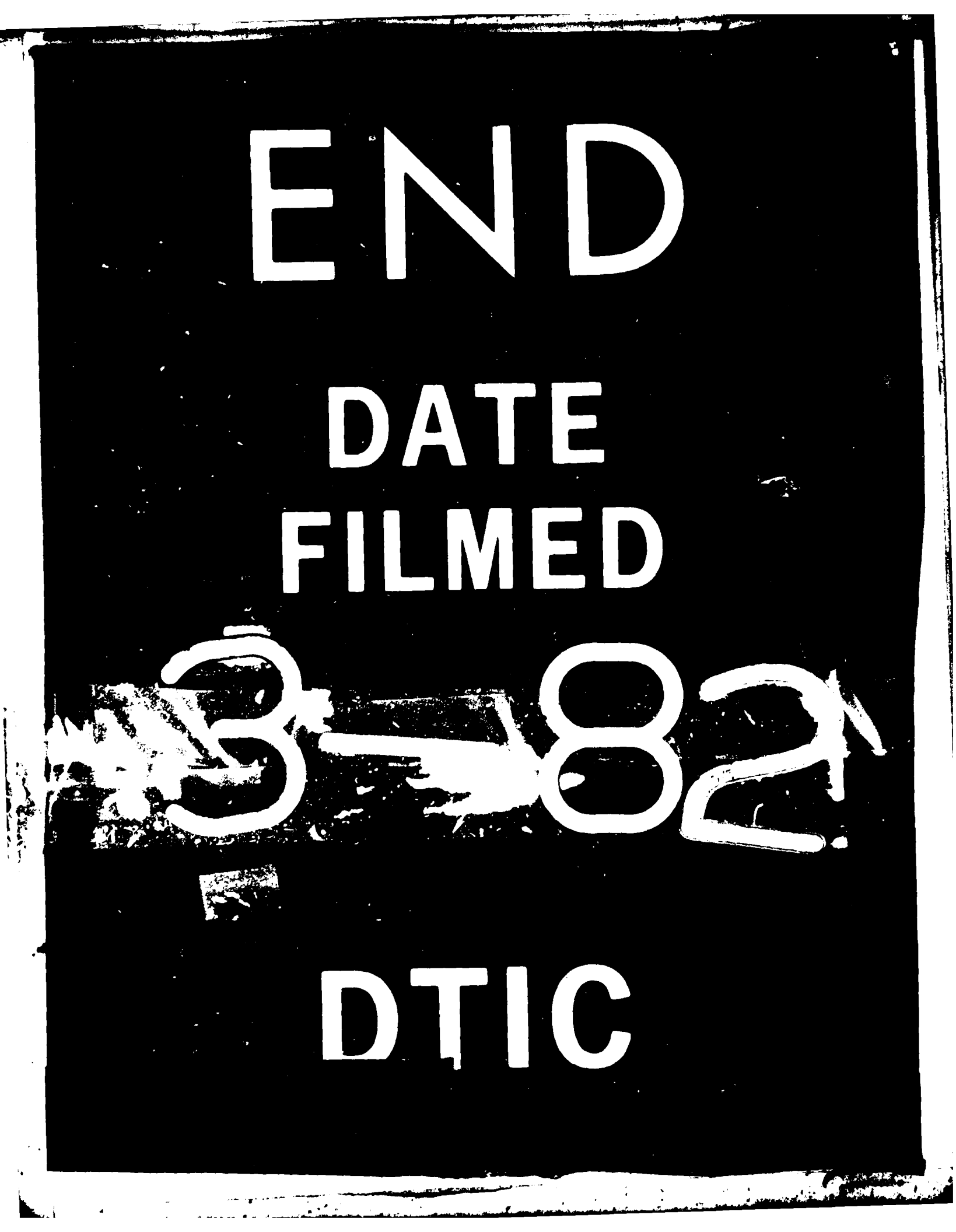
END
DATE
FILMED
3-82
DTIC